Automated Mathematical-Based Rigging Design System for Heavy Industrial Modules

Seyedmohammadamin Minayhashemi

A Thesis

In the Department

of

Building, Civil, and Environmental Engineering

Presented in Partial Fulfillment of the Requirements

For the Degree of

Master of Applied Science (Civil Engineering) at

Concordia University

Montreal, Quebec, Canada

October 2019

Concordia University

School of Graduate Studies

This is to certify that the thesis prepared

By: Seyedmohammadamin Minayhashemi

Entitled: Automated Mathematical-Based Rigging Design System for Heavy Industrial Modules

and submitted in partial fulfillment of the requirements for the degree of

Master of Applied Science (Civil Engineering)

Signed by the final Examining Committee:

_____Chair

Dr. M. Nik-Bakht

_____Examiner

Dr. A. Hammad

_____Examiner

Dr. F. Nasiri

_____Supervisor

Dr. S. H. Han

Approved by_____

Dr. Michelle Nokken, Graduate Program Director

October 31, 2019 _____

Dr. Amir Asif, Dean, Gina Cody School of Engineering and Computer Science

Abstract

Automated Mathematical-Based Rigging Design System for Heavy Industrial Modules

Seyedmohammadamin Minayhashemi

Modular-based heavy industrial construction projects typically involve the use of mobile cranes to lift and place large heavy prefabricated modules. These modules must be lifted vertically, raised evenly, and maintained in a level position during the lift in order to prevent them from deflecting and, more importantly, to mitigate safety issues regarding potential rigging failure. In this respect, a comprehensive crane lift study at the planning stage of the project is required to ensure the lifts are successful and to improve safety and productivity. One of the most tedious and time-intensive tasks involved in conducting the lift study is the design of the rigging assemblies, which are the link between the crane hook and the module. In practice, however, this task is performed manually and relies heavily on guesswork, which is error-prone and time-consuming, especially when the center of gravity is offset from the center of the module. Poorly designed rigging assemblies are only detected at the job site when the module does not raise evenly at the beginning of the lift, which then results in wasted time and productivity loss as the assembled components have to be unrigged and properly adjusted. To overcome these limitations, this thesis proposes an automated mathematical-based rigging assembly design system that consists of: *(i)* the solver analysis, which calculates the sling angles and performs the calculations required to balance the module; *(ii)* the rigging assembly designer, which determines the required capacity of the rigging components and selects the suitable riggings from the database; *(iii)* the 3D visualizer,

which creates a 3D model of the designed rigging assembly. This framework enables lift engineers to create rigging assembly designs more precisely and expeditiously. The methodology is validated in a case study.

Acknowledgements

First and foremost, I would like to express my deepest gratitude to my supervisor Dr. SangHyeok Han for his constructive comments and warm encouragement on this work.

I would also like to show my greatest appreciation to Dr. Ahmed Bouferguene at the University of Alberta. The door to his office was always open whenever I ran into a trouble spot or had a question about my research.

Special thanks to Dr. Jacek Olearczyk and Mr. Joe Kosa, my supervisors at NCSG Engineering Ltd, who gave me all the freedom to pursue my research at the company.

I am indebted to my parents for their unconditional love and support in my journey to get my Master's degree and at every stage of my life.

And finally, last but by no means least, I cannot find words to express my gratitude to my beloved wife. Without her endless patience and support I could not imagine finishing my Master's degree.

Table of Contents

Table of Figures

Table of Tables

Table of Parameters

Parameter	Description
a,b,c	Sides of the triangle (Fig. 8)
C_i	Inside length of i shackle (Eq. (16))
f	Minimum absolute difference between the required amount of increase and the total length made by the chain of shackle (Eq. (16))
F_{L1}, F_{R1}	Sling forces at the first level of the rigging assembly (Fig. 13)
F_{L2}, F_{R2}	Sling forces at the second level of the rigging assembly (Fig. 13)
$H_{Desired}$	Desired total height of the 2-point pick segment (Eq. (23)
H_{Remain}	Remaining height (Eq. (23)
H_{Slings}	Total height of slings in the 2-point pick segment (Eq. (23)
H_W	Width of the hook (Fig. 8)
$Max(SL_{DB})$	Maximum sling length available in the database (Fig. 14)
$Max(TB_L)$	Maximum opening length of the turnbuckles available in the database (Fig. 14)
$Min(SL_{DB})$	Minimum sling length available in the database (Fig. 14)
$Min(TB_L)$	Minimum opening length of turnbuckles available in the database (Fig. 14)
N	Total number of shackles available with different sizes (Eq. (16))
n_i	The number of i shackles used in the chain (Eq. (16))
$ofst$	COG offset from the lifting point (Fig. 8)
RAI	Required Amount of Increase (Fig. 6)

S_B	Distance from the right/left side of the spreader bar to the lifting point on the right/left side (Fig. 8)
SB_L	Length of the spreader bar (Fig. 8)
SB_{Lx}	Horizontal projection of SB_L (Fig. 8)
S_L	Distance from the left side of the spreader bar to the left side of the hook (Fig. 8)
SL_{1st}	Sling length at the first level of the 2-point pick segment (Eq. (23)
SL_{2nd}	Sling length at the second level of the 2-point pick segment (Eq. (23)
SL_{3rd}	Sling length at the third level of the 2-point pick segment (Eq. (23)
S_{Lx}	Horizontal projection of S_L (Fig. 8)
S_R	Distance from the right end of the spreader bar to the right side of the hook (Fig. 8)
S_{Rx}	Horizontal projection of S_R (Fig. 8)
W_L, W_R	Weight forces applied to the lifting points (Fig. 13)
x	Distance from the right side of the hook to the vertical line crossing the COG (Fig. 8)
α	Angle of sling attached to the bottom right of the spreader bar with the vertical line (Fig. 8)
β	Angle of sling attached to the bottom left of the spreader bar with the vertical line (Fig. 8)
γ	Slope of the spreader bar (Fig. 13)
δ	The angle of plane which contains the slings and the spreader bar at the second level with the vertical plane (Fig. 13)
θ_L	Angle of sling attached to the top left of the spreader bar with the spreader bar (Fig. 8)
θ_R	Angle of sling attached to the top right of the spreader bar with the spreader bar (Fig. 8)
σ	Angle of sling attached to the top left of the spreader bar with the horizontal line (Fig. 8)

Chapter 1: Introduction

Modularization is a growing trend in construction thanks to its efficiency in terms of time, cost and quality improvement [1]. This mode of construction thus is the solution of choice for heavy industrial projects, especially oil refinery facilities, in the province of Alberta, Canada. In these projects, hundreds of modules are prefabricated in a controlled environment, transported to the job sites, lifted from their pick locations, and finally erected in their planned position. These modules which have *N* lifting points (4 to 16 lifting points depending on the module length) can typically be classified as pipe racks, cable trays and building modules [2]. Furthermore, their weights are up to 160 tons with the following dimensions: (*i*) up to 7.3 m (24 ft.) in width; (*ii*) 42 m (138 ft.) in length; and (*iii*) 8.4 m (27.5 ft.) in height [4].

In order to prevent the modules from tilting, they are required to be lifted vertically and evenly from the extension of the module's columns which are located on the top of the modules. Lifting the modules unevenly can potentially result in deflecting them and, more importantly, due to unexpected distribution of the load throughout the rigging assembly, increase the risk of rigging failure, thus lifting safety issues. At this junction, it should be noted that, rigging failure is one of the major causes of crane accidents. According to a study based on the Occupational Safety and Health Administration (OSHA) database, 28.1% of the fatal crane accidents happened in the United States from 2002 to 2012 caused by failure of wire ropes, slings and hoist lines. The other causes of fatal crane accidents were overturn/tips (8.6%), collapse (11.4%), ground conditions (3.6%), power line contact (5.6%), overloading/unstable (26%), signal/communication error (9.4%), and others (7.3%) [5].

Rigging assemblies are generally used to not only build physical connection between the

crane's hook and the modules but also determine how the load is distributed from the lifting points to the crane's hook. Suitably designed rigging assemblies have a vital role in successfulness of the lift and can make sure the modules are lifted safely and efficiently.

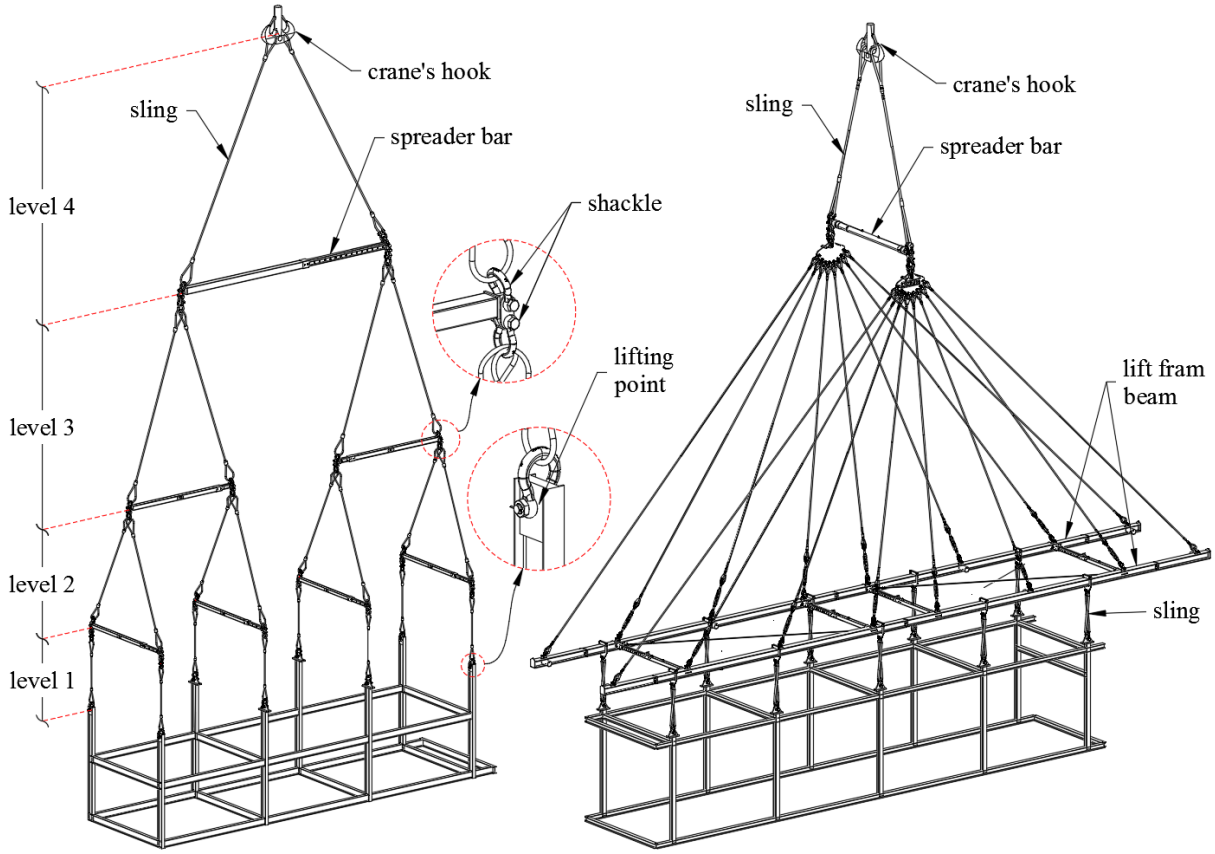

Fig. 1. Traditional rigging assembly and lift frame

As shown in Fig. 1, two types of rigging assemblies are currently used for lifting heavy industrial modules:

i. Traditional rigging assemblies (Fig. 1(a)) which are a combination of spreader bars, slings and shackles that are used to transfer pairs of loads from the lifting (pick) points of the module to the crane's hook using triangular slinging arrangements. The term "level" is used in this thesis to refer to the rigging components used at different heights of the

assembly. The number of levels in traditional rigging assemblies vary based on the number of module's lifting points.

ii. Lift frames (Fig. 1(b)) which are the newly emerged alternative to traditional rigging assemblies. In lift frames, the load is firstly transferred from the lifting points to two long beams running along the length of the module. A single spreader bar then transfers the load from the two beams to the crane's hook.

The design process for traditional rigging assemblies is laborious and time-consuming to assemble compared to the lift frames [2]. The number of rigging components in traditional rigging assemblies may reach to 150 pieces for large modules [3]. However, this technology is still widely used in practice because project owners and lifting contractors are very familiar with the solutions that need to be implemented to circumvent any potential challenge that may unexpectedly occur on the construction site. Moreover, the lift frames are 30 to 40% heavier than the traditional rigging assemblies depending on the size of the module to be lifted. In addition, as shown in Fig. 1(b), the length of lift frame beams may exceed the module's length which increases the risk of collision with crane's boom as well as other site obstacles. It should be noted that this thesis focuses on overcoming the limitations of designing traditional rigging assemblies using an automated procedure which integrates rigging analysis calculations with 3D visualization.

As mentioned earlier, unevenly lifting a module not only involves safety issues regarding rigging failure but also increases the risk of damage to the structural components of the module. To solve this issue, in practice, the assembled rigging components need to be unrigged and adjusted properly to balance the load which leads to reduce lifting productivity due to waste of design and lifting times. In this respect, designing a rigging assembly which ensures the module is lifted

evenly and maintained in a level position during the lift is paramount.

The design process used to assemble rigging system consists of the following tasks:

i. Calculating the required capacity of each rigging component based on the module information such as its weight, dimensions, the Center Of Gravity (COG) position, and number of lifting points.

ii. Selecting suitable rigging components from their capacity charts based on the required capacities and dimensions;

iii. Calculating the total weight of the rigging assembly which is used in crane selection.

iv. Creating a 3D model of the rigging assembly to identify whether the selected rigging components can actually be used together (size compatibility of the selected rigging components). The developed 3D model, as a part of a more comprehensive 3D lift study, is then used to ensure that the module and rigging assembly do not collide with crane's boom and/or site obstacles.

Manually performing these tasks, especially when the COG is offset from the center of the module, is a tedious and error-prone process relying heavily on guesswork which can take from 0.5 to 4 hours per module depending on the number of lifting points on the modules as well as the engineer's experience.

To overcome these limitations, this thesis proposes an automated mathematical-based rigging assembly design system which consists of: *(i)* collecting module and available rigging component information; *(ii)* a solver analysis which calculates the sling angles and performs the required calculations for balancing the module; *(iii)* rigging assembly designer which determines

the required capacity of the rigging components and selects the suitable riggings from the database; *(iv)* rigging assembly design alternatives; and *(v)* 3D visualizer which creates a 3D model of the designed rigging assembly. The proposed system is developed in AutoCAD platform using Application Programming Interface (API).

Chapter 2: Literature Review

A significant number of researches have been done in the area of heavy lift studies to address issues regarding crane selection [[4], [6]-[8]], crane lift path planning [[9]-[12]], and crane operation simulation [[13]-[16]]. On the other hand, research on the development of design frameworks for crane rigging assemblies has received less attention in both academia and industry despite their importance for safety and efficiency. In practice, rigging assembly design is time-consuming and error-prone and is often associated with loss of productivity and safety reduction.

One common slinging arrangement for lifting modules referred to as 4-point pick modules, consists in attaching 4 diagonal slings directly from the lifting points to the hook (Fig. 2). In the ideal scenario where the COG is exactly at the center of the module, the length of the slings used to transfer the load from the module to the crane's hook in a 4-point pick scenario need to be exactly equal (assuming the pick points are distributed symmetrically with respect to the COG). In practice, however, because the COG is likely to be offset from the geometric center of the module, the length of the slings need to be adjusted in order to have a balanced transfer of the load which will ensure that the lifted module stays level at all time. Moreover, the alignment of the lifting lugs, which are the most vulnerable places of the module [17], is important in this configuration. Each of the lifting lugs must be in plane towards the COG (Fig. 2(a)). If the lifting lugs are aligned toward X axis direction (Fig. 2(b)), the load is not applied on the shackles in-line due to the angle that slings make with the shackles (α) which referred to as side-loading [18] . In that case, the working load limit of the shackle must be reduced based on the angle of sling with shackle according to its supplier's manual. The working load limit of the shackle may be reduced to as low as 50% of its full capacity in side-loading applications [19]. Considering the uncertainties

in the position of COG, length of slings and the angle of slings with shackles, Anderson [18] suggests to design the lifting lugs, shackles, and slings in a way that two of them are able to carry the entire load.

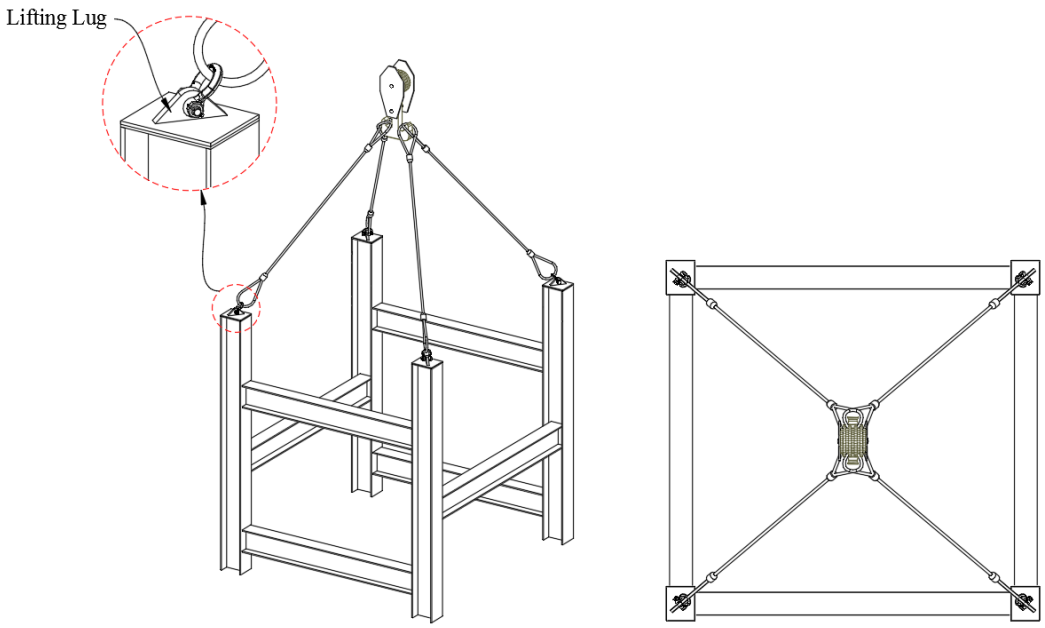

(a)

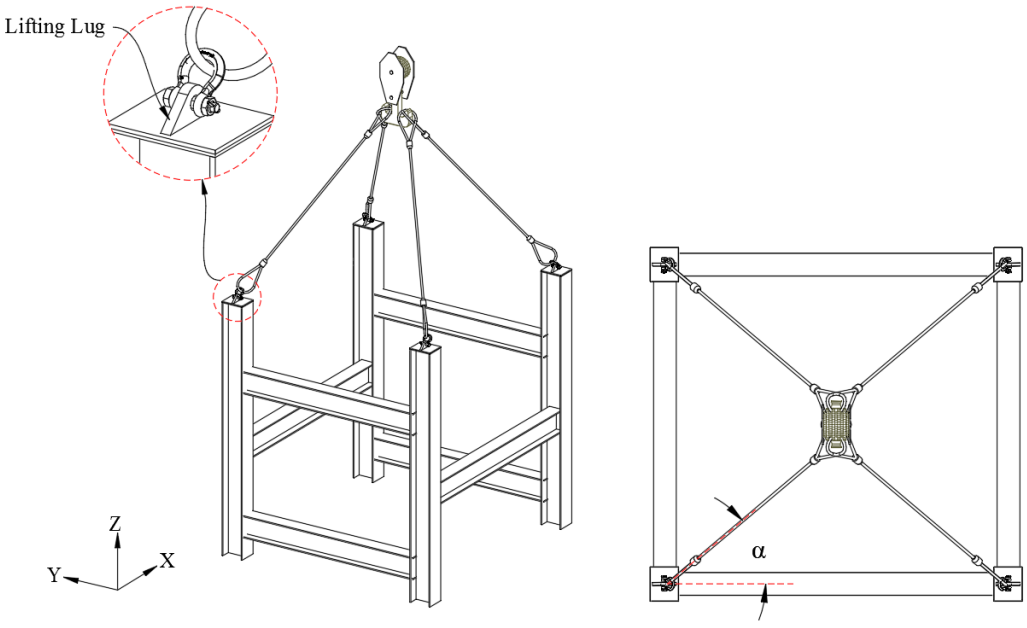

(b)

Fig. 2. 4-point pick rigging assembly with diagonal slings

In previous work, Sam [20] developed a spreadsheet to determine the load distribution between the 4 slings considering the position of COG and sling lengths. The position of each lifting point, length of slings and the COG position of the module are the inputs of his study whereas the width of the hook is not considered due to its insignificant effect on the sling load and distribution. The scope of Sam's study is limited to 4-point pick modules unless an independent and separate analysis is done for the modules that have more than 4 lifting points and are lifted with multiple cranes.

Lifting points of modules may be located at the bottom of the modules. Lifting from bottom, however, involves risk of instability if the module's COG is too high as it may be dumped in the course of its motion. In this respect, for 4-point pick modules which are required to be lifted from their bottom, an analytical necessary and sufficient criterion for Lyapunov stability or asymptotic stability was suggested by Longman and Freudenstein [21]. They defined an expression for the margin of stability in which the disturbance forces caused by crane hook motion during the lift can be tolerated. Their methodology cannot be applied on modules with more than 4 lifting points.

Unless required by the size of the payload, e.g. long vessels, wind turbine propellers, etc., which necessitates vertical orientation at the set point single crane lifts operations are generally preferred to their tandem crane counterparts since the risk associated with the former is lower in comparison to the latter [7]. In this regard, Chen et al. [22] suggested a numerical model for manipulating the angle of twin-hoisted objects using one crane. In their model, the hoist lines of the boom and auxiliary jib need to be adjusted to accommodate the desired object angle during the lift. However, this model can only be used to control the object angle in one direction. In addition, the available capacity of the crane becomes more limited when crane's auxiliary jib is used which

is necessary in their model.

As described in previous section, compared to the other research areas regarding heavy lift studies (crane selection, crane lift path planning, crane operation simulation, etc.) there are relatively less researches and/or practical reports in terms of methods to support the design of rigging components. However, there are a few commercial software that can help designing rigging assembly.

Industry-academic researches and developments have led to computer-aided heavy lift planning systems in order to assist lift engineers in the planning phase of the heavy lift projects. A Computer-Aided Rigging (CAR) system was developed by Brown & Root company which reportedly integrates basic rigging analysis and documentation of rigging plans in a CAD platform [23]. At Bechtel, a heavy lift planning and visualization software called Automated Lift Planning System (ALPS) was developed for crane selection, rigging assembly design and 3D simulation features [24]. At the University of Texas at Austin, a Heavy Lift Planning System (HeLPS) was built in order to facilitate tasks such as determining crane location, ground support and lift path clearances. HeLPS employed a 3D visualization package called as Walkthru which was also developed in the MicroStation environment [25]. Other standalone pieces of software such as 3D Lift Plan [26], CRANEbee [27] and kranXpert [28] have been commercially available. However, these software programs have yet to fully succeed in terms of being widely adopted due to the following reasons: (i) they assist lift engineers to design rigging configurations manually or semi-manually; and (ii) they may result in wasted assembly time on-site since actual rigging components (e.g., slings, spreader bars, and shackles) are represented by the software programs as simple solid geometries, which are not capable of indicating size incompatibilities between rigging components

that may result in the components not being able to be assembled in real life

In order to overcome these limitations, this thesis presents a mathematical-based rigging assembly design system which automates the design of rigging assemblies for a large number of modules which are generally used in heavy industrial construction projects. The proposed system consists of: *(i)* collecting module information; *(ii)* automating the rigging analysis calculations; *(iii)* reporting the result of analyses; and *(iv)* visualizing the rigging assembly in 3D environment. Moreover, the proposed framework provides rigging assembly information (e.g., overall heights and weights) as one of the results from the proposed system which is an essential input to complete the crane selection, crane lift path planning, and crane operation simulation successfully and efficiently.

Chapter 3: Proposed Methodology

The proposed methodology for an automated mathematical-based rigging assembly design system is illustrated in Fig. 3.

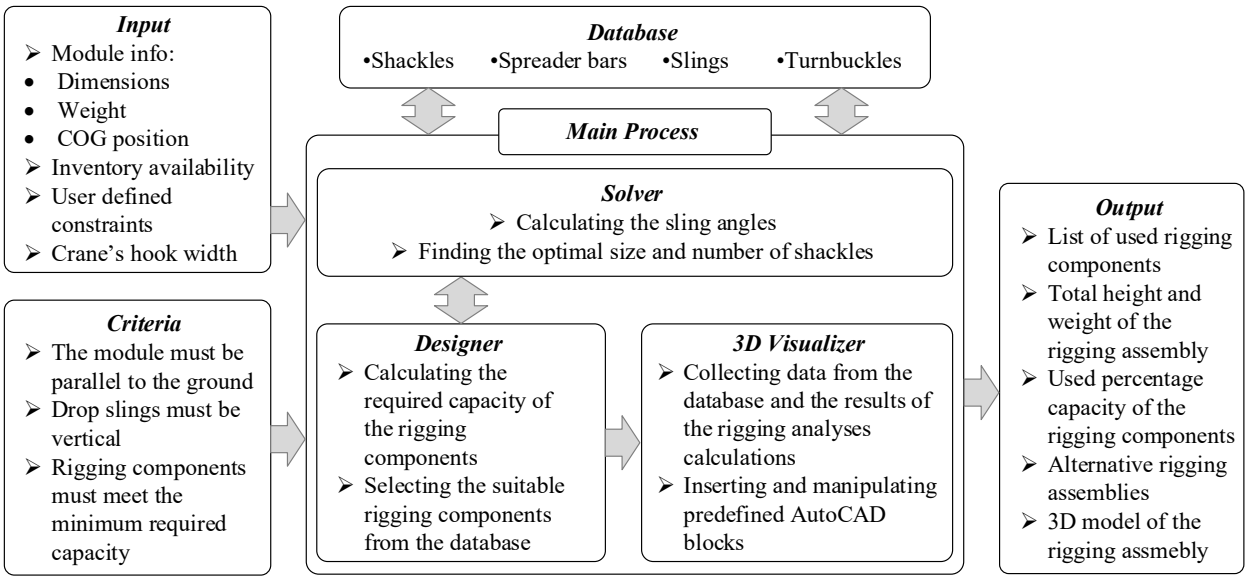

Fig. 3. The proposed methodology

The required input data which need to be entered manually by the user consists of:

i. Module information including dimensions, weights, and the COG position.

ii. Availability of rigging components in inventory such as shackles, spreader bars, slings, and turnbuckles

iii. User defined constraints such as maximum acceptable angle of drop slings

iv. The crane hook's width.

The design criteria are:

i. The module must be lifted evenly and maintained in a level position during the lift. In other

words, the lifted module must be parallel to the ground. Otherwise, the load is unexpectedly distributed throughout the rigging assembly and, in consequence, potential rigging failure and module deflection may be occurred

ii. The angle between the drop slings (slings at the first level of the rigging assembly attached to the lifting points) and the module must be perpendicular so that only vertical tension forces are applied on the module's columns which prevents the module from bending

iii. The selected rigging components must meet the minimum required capacity.

Failure to meet each of these criteria could jeopardize the safety during the lift.

Based on the input and criteria, the proposed methodology to design rigging assembly for each of the modules involves mainly three modules:

i. ***Solver*** which performs two tasks: First, calculating the sling angles at each level of the rigging assembly through solving a system of nonlinear equations; and second, finding the optimal size and number of shackles, which are attached to slings to increase their lengths, to satisfy the criteria *(i)* and *(ii)*

ii. ***Designer*** which calculates the required capacity of the rigging components based on the module information and selects suitable rigging components that meet the required capacity from the data considering their availability in the inventory.

iii. ***3D visualizer*** which creates a 3D model of the rigging assembly in the AutoCAD platform using AutoCAD Application Programming Interface (API). Creating the 3D model is an essential step to identify size compatibility of the selected rigging components which means whether the selected rigging components can actually be used together. If an

incompatibility issue is encountered, the user may choose to put constraints on the availability of the rigging components that cause the error and start the design over again, or to perform the required modifications manually. Moreover, as mentioned earlier, the developed 3D model is used to ensure that the module and rigging assembly do not have collision risks among crane's boom and/or site obstacles. The 3D visualizer module collects the required data from both the database and the results of the rigging analyses. The collected data is then used in inserting and positioning the rigging components which are stored as AutoCAD 3D blocks in the database.

Finally, the outputs of the system are mainly rigging designs (can be more than one single design) which involve a list of selected rigging components, total height and weight of the rigging assembly and proposed percentage capacity of the rigging components in accordance with alternatives of the rigging assembly designed by the proposed methodology. The proposed methodology which is developed using C# language assists lift engineers to design the rigging assemblies automatically and efficiently for safe lifting.

Before describing more detail information for each of the three modules, the slinging arrangement of modules with *N* lifting points (4 to 16 lifting points) and the concept of sling length adjustment are described in the following sections.

3.1 Slinging Arrangement of Modules with *N* Lifting Points

As mentioned earlier, industrial modules may have *N* lifting points (4 to 16 lifting points depending on the module length). Fig. 4 shows an industrial 12-point pick module during the lift using traditional rigging assembly. Rigging assembly of these modules are designed with combining 4-point pick and 2-point pick segments as shown in Fig. 5.

Fig. 4. Lifting an industrial 12-point pick module

4-point rigging assemblies are a fundamental segment in the rigging assembly of the modules. They consist of 3 spreader bars; two of which are along the Y-axis and the other is along the X-axis. The load is generally transferred from the lifting points to the hook or to the end of the spreader bar located at the higher level. For instance, the 4-point pick segment that is used in 6-point pick rigging assemblies transfers the load from the lifting points to the hook; and the 4-point pick segments used in 8-point pick rigging assemblies transfer the load from the lifting points to the end of the spreader bar located at the level 4.

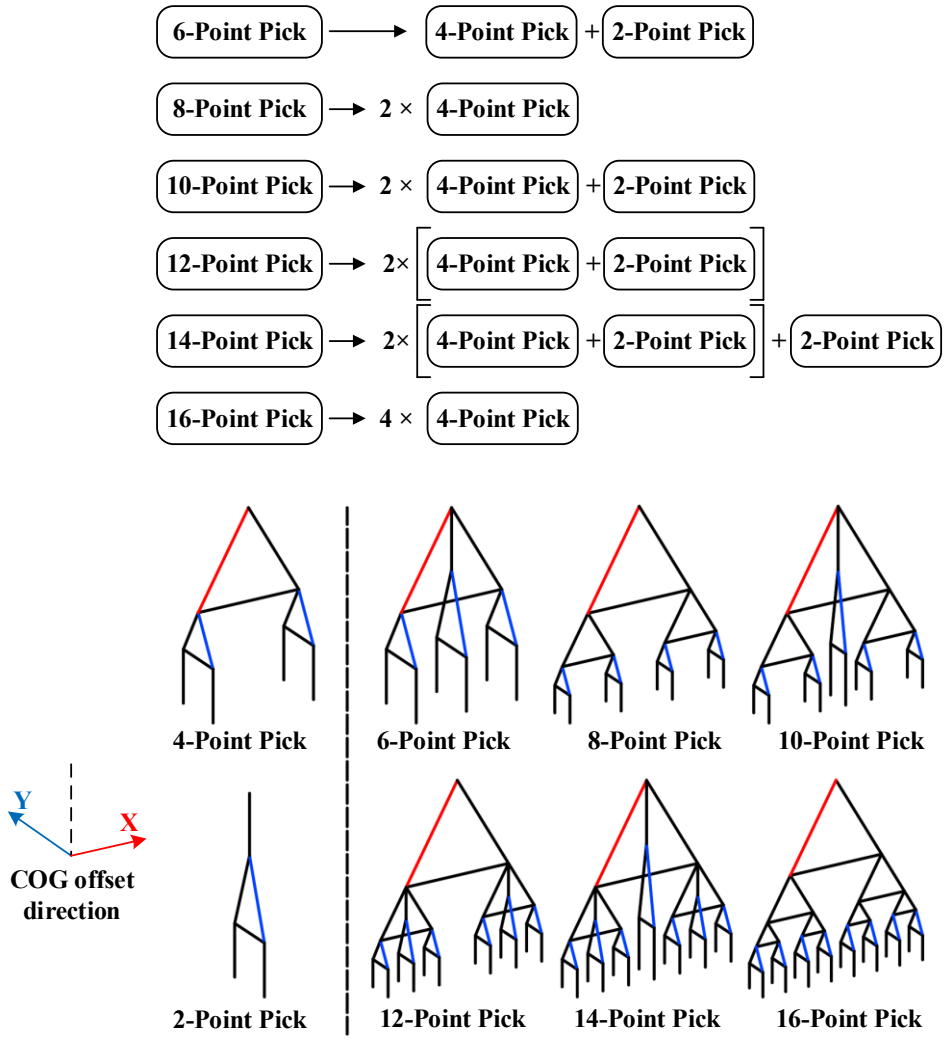

Fig. 5. Slinging arrangement of modules with *N* lifting points

2-point pick segments, which use only one spreader bar along the Y-axis of the module, are applied in the rigging assembly of the modules with 6, 10, 12, and 14 lifting points. These segments are utilized either inside of the 4-point pick segments for the modules which have 6, 12, and 14 lifting points or in the middle of the whole rigging assembly for the modules which have 10 and 14 lifting points. In this respect, this thesis describes the concepts of the rigging design which are 2-point pick and 4-point pick segments instead of covering all of possible pick points.

3.2 Sling Length Adjustment

The length of slings used in the rigging assemblies needs to be adjusted for two main purposes: *(i)* balance the module which must be parallel to the ground during the lift; and *(ii)* make sure that all of the slings are taut and not slack so that they can have responsibility in terms of the assigned load. The adjustments of the sling length are generally implemented by mounting a chain of shackles or a turnbuckle to one end of the sling on where the imbalance of the load is existed.

When the COG is offset from the Center Of the Module (COM) in order to balance the load in both X and Y direction, sling length adjustment is required at different levels of the rigging assembly in accordance with X and Y axis. With respect of balancing the load in X direction, the length of the sling, which is located on the opposite direction of the COG offset represented as red lines in Fig. 5 at the highest level of the configuration, is increased. In order to balance the load in Y direction, all of the slings on the opposite direction of the COG offset at the lowest level illustrated as blue lines in Fig. 5 are lengthened.

For example, as shown in Fig. 6(a), the vertical line crossing the COG is on the right side of the COM, meaning that the COG is offset to the positive X direction. Therefore, to balance the load in X direction, the length of sling on the left side and above the spreader bar must be increased

by a specific amount, referred to as the Required Amount of Increase (RAI). It is worth mentioning that, two slings above the spreader bar are always identical in length. Therefore, a chain of shackles is used to take up the amount of slack between the sling end and the shackle attached to the spreader bar (i.e. RAI) on the left side. The calculation of the RAI, and determining the size of number of shackles are completed by the solver module.

In attaching additional shackles above the spreader bars, it should be noted that, the first shackle that is attached to the spreader bar's shackle, is used upside down with a bow-to-bow connection (Fig. 6 (b)) to avoid potential interference between the shackle's pin and the spreader bar's body. The next shackles in the chain could have any type of point-to-point connection including bow-to-bow, pin-to-pin or pin-to-bow. It must be checked if the shackles are allowed to be used in a point-to-point loading according to the supplier's manual since not all the shackles are designed for this application.

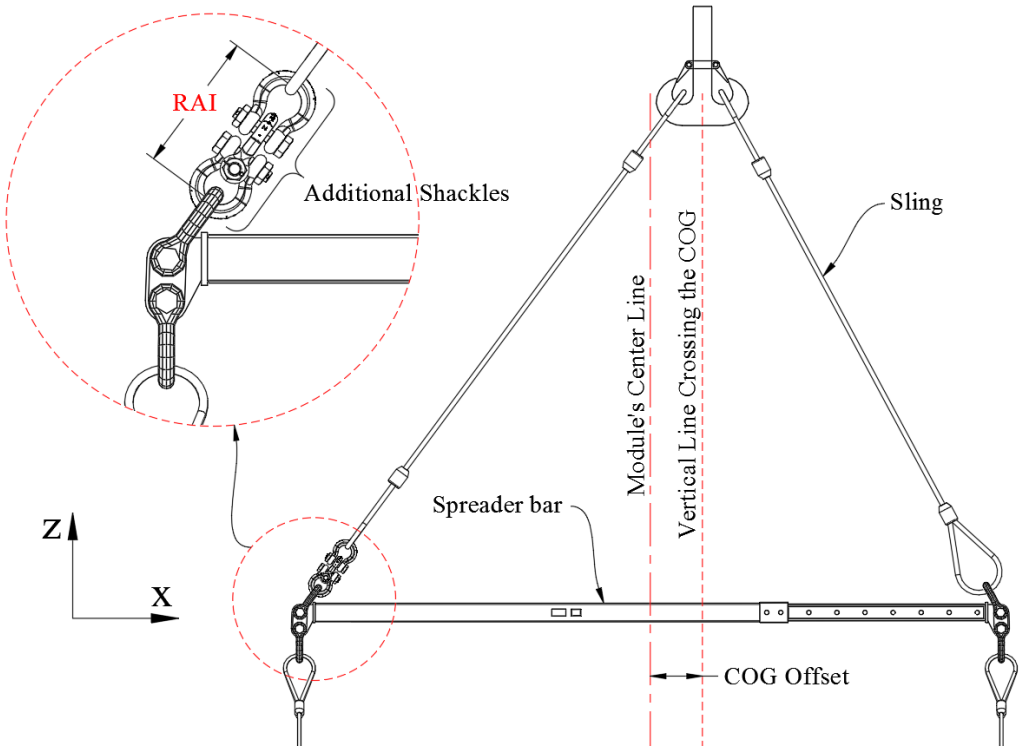

(a)

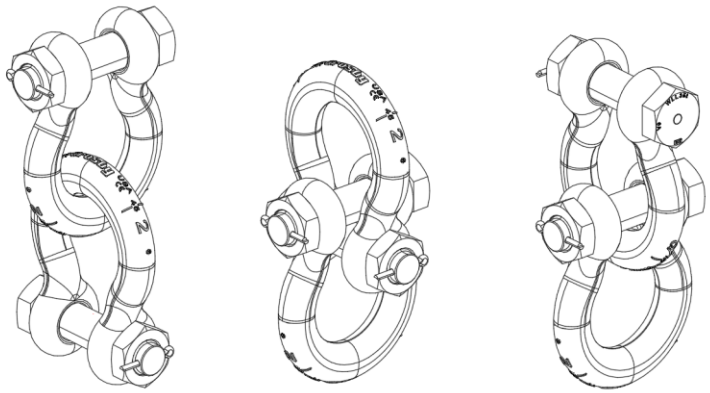

bow-to-bow pin-to-pin pin-to-bow

(b)

Fig. 6. Sling length adjustment to balance the load with the chain of shackles

When a 2-point pick segment is used in rigging assemblies, in order to make sure that all the slings in this segment take the load, the total height of the 2-point pick segment must be adjusted to accommodate: *(i)* the height of the 4-point pick segments when it is located inside of the 4-point pick segments; and/or *(ii)* the height of the whole rigging assembly when it is located in the middle of rigging assembly. Depending on the location of this segment in various *N*-point pick modules, these conditions should be satisfied, accordingly. In this respect, as illustrated in Fig. 7(a), the height of 2-point pick is adjusted by changing the length of turnbuckles mounted to the end of drop slings based on a minimum or maximum opening length shown in Fig. 7(b). In selecting turnbuckles, it is important to verify if the turnbuckle has enough length to take up the slack between the end of drop sling and the shackle attached to the lifting point. The algorithm of configuring 2-point pick segments will be explained in the designer module.

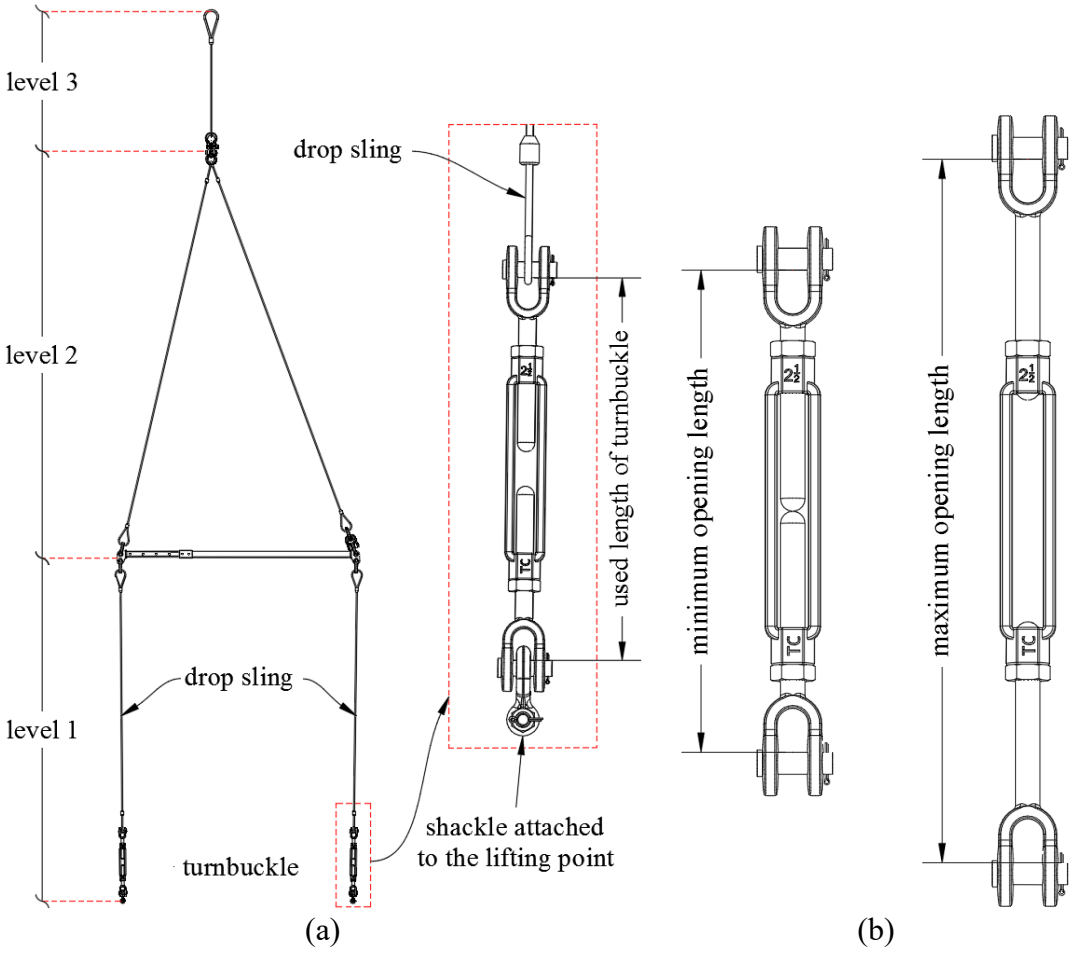

Fig. 7. Sling length adjustment using turnbuckles in 2-point pick segments

3.3 Solver Module

The solver module is called within the main process of the proposed system to perform two tasks: *(i)* calculating the sling angles and the *RAI* in the length of one of two slings above the spreader bar for balancing the load through solving a system of 11 equations when the COG is offset in X and/or Y direction. *(ii)* finding the optimal size and number of shackles that make a total length which must be satisfied by as close as possible to the *RAI*.

3.3.1 Task 1

The sling angles at each level of the rigging assembly and the *RAI* are calculated in a two-dimensional plane involving the spreader bar and the two slings above it. A 4-point pick rigging assembly, which is a fundamental segment in rigging assemblies of heavy industrial modules, is used to describe the parameters that are required in finding the sling angles and the *RAI*. Fig. 8 represents 4-point pick rigging assemblies where the length of the spreader bar at level 3 is longer (Fig. 8(a)) or shorter (Fig. 8(b)) than the length of the module and the COG is offset from the center of the module in positive X direction. If the actual COG is offset into negative X direction, the same amount of offset from the module's center is assumed to be in positive X direction and the results of the designed rigging assembly are mirrored about XZ plane. In Fig. 8, the difference between the length of spreader bar and the distance between the lifting points has been exaggerated in order to show the angles more clearly. In practice, however, the spreader bars' length is adjusted by specific intervals to accommodate the distance between the lifting points on the module.

In setting up the equations by which the sling angles and the *RAI* are calculated, six known parameters and three geometrical constraints are required initially. The known parameters are as follows:

1. Width of the hook (H_W).
2. Distance between the two end lifting points (M)
3. COG offset from the lifting point ($ofst$)
4. Length of the spreader bar (SB_L)
5. Distance from the right end of the spreader bar to the right side of the hook (S_R)
6. Distance from the right/left side of the spreader bar to the lifting point on the right/left side (S_B).

These parameters are determined by the user, module information, and results of a preliminary design in which the COG is assumed to be at the middle of the module. The preliminary design is performed by the designer module which will be explained later. The geometrical constraints employed in setting up the equations are:

1. The extension of inclined lines above and below the spreader bar (illustrated as blue dash lines in Fig. 8) must intersect each other on the vertical line crossing the COG (illustrated as red dash lines in Fig. 8) to establish the equilibrium of the module and the rigging configurations based on balancing forces which are the module's weight force acting vertically through the COG and the forces acting on the slings located in above and below the spreader.
2. The line M must be balanced horizontally to satisfy the design criteria *(i)* described above
3. The line H_W must be balanced horizontally since the crane's hook is only rotated along Z axis.

It is worth mentioning that, if the COG is offset from the module's center, the spreader

bar has inevitably a slight slope when the module and spreader bar are not equal in length.

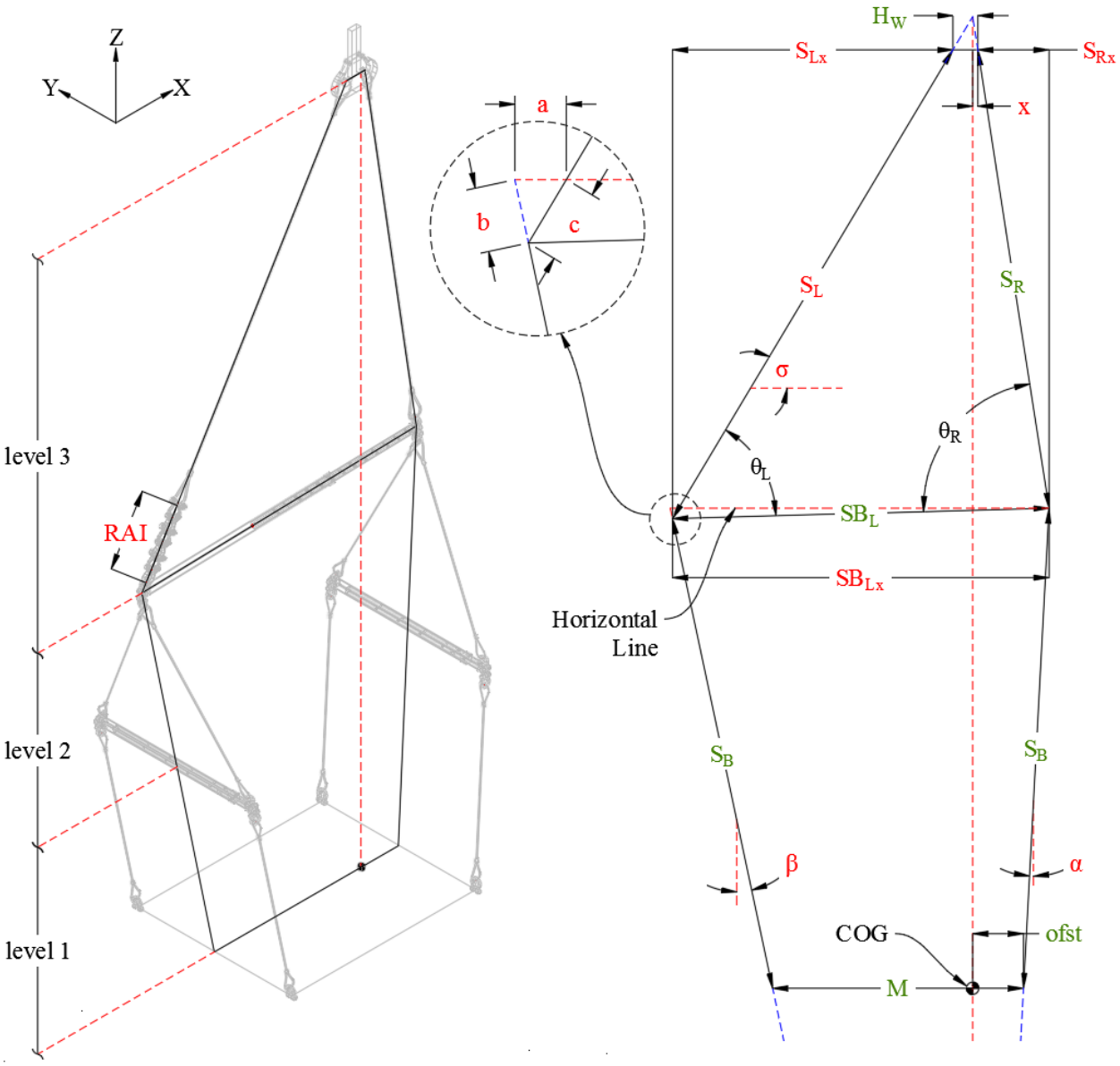

(a)

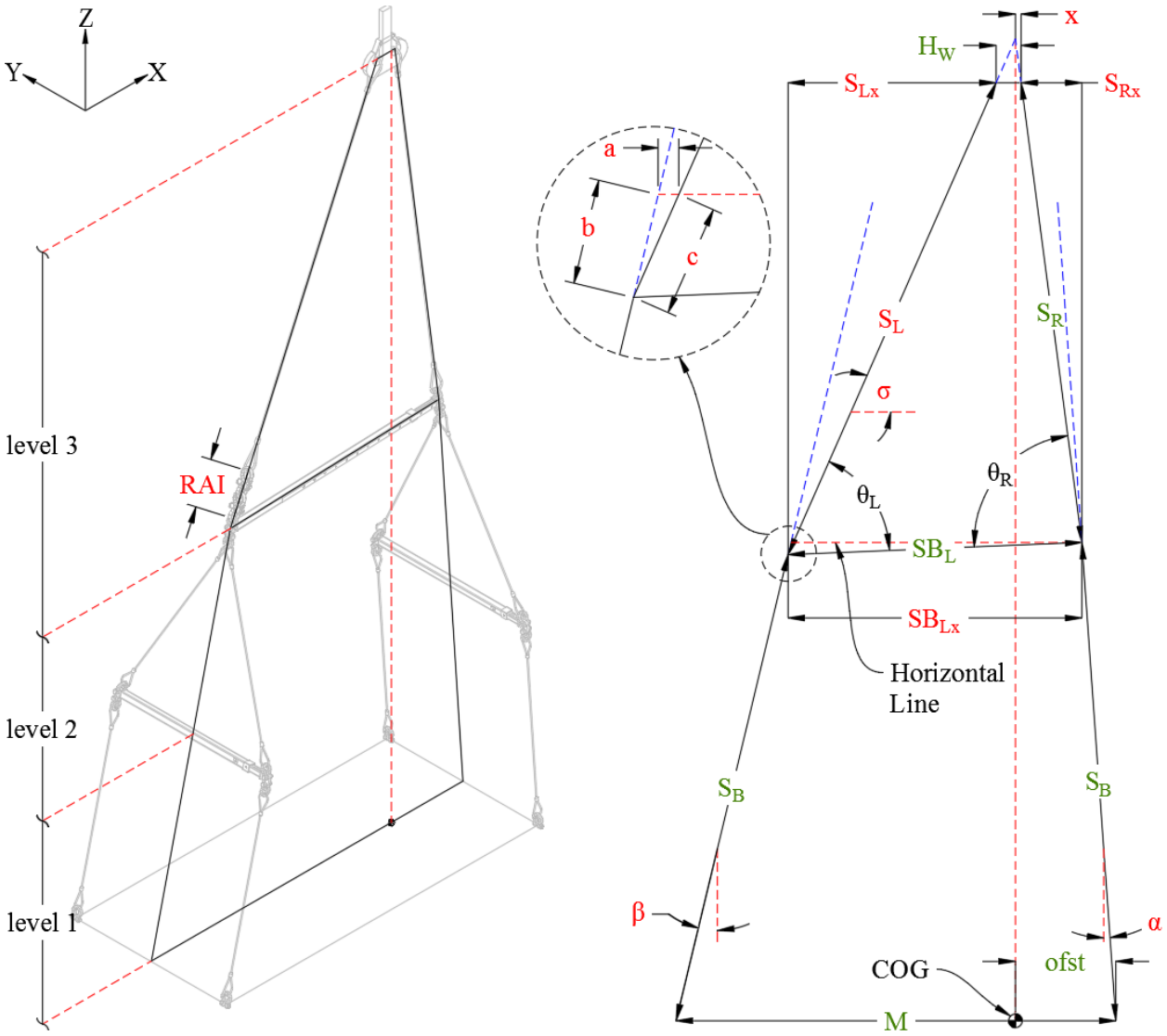

(b)

Fig. 8. Two-dimensional drawing of a 4-point pick rigging assembly

As the calculation of sling angles and the *RAI* involves more than one unknown parameter, they cannot be determined directly. That is, other unknown parameters are required to be determined prior to calculating the sling angles and the *RAI*. In this regard, there are 11 unknown parameters which are: distance from the right side of the hook to the vertical line crossing the COG (x); distance from the left side of the spreader bar to the left side of the hook (S_L), horizontal projection of S_L (S_{Lx}), horizontal projection of S_R (S_{Rx}), horizontal projection of SB_L (SB_{Lx}); and α,

β, σ, a, b, and c as shown in Fig. 8. The unknown parameters are solved in a system of equations where all the equations must be satisfied simultaneously. Previous work [29] used Wolfram Mathematica kernel to solve the system of equations efficiently and effectively for the same problem. Since this kernel is required many times leading to slow down the process time of the proposed system, this thesis develops an algorithm to solve the system of equations within the same manner in order to correspond to one of objectives in this thesis, efficient rigging configuration design both on-site and during the design phase of construction projects in a short manner.

It should be noted that, in any of the following equations that the symbols $\pm, \mp$ are used, the upper operator is chosen for Fig. 8(a) where the spreader bar is longer than the module's length; and the lower operator is chosen for Fig. 8(b) where the spreader bar is shorter than the module's length. In order to make it easier to follow the equations, Fig. 9 and Fig. 10 are provided to illustrate the terms that are used in the equations for the upper and lower part of the Fig. 8 respectively. Fig. 9(a) and Fig. 10(a) are used for the case that the spreader bar is longer than the module's length; and Fig. 9(b) and Fig. 10(b) are used for the case that the spreader bar is shorter than the module's length.

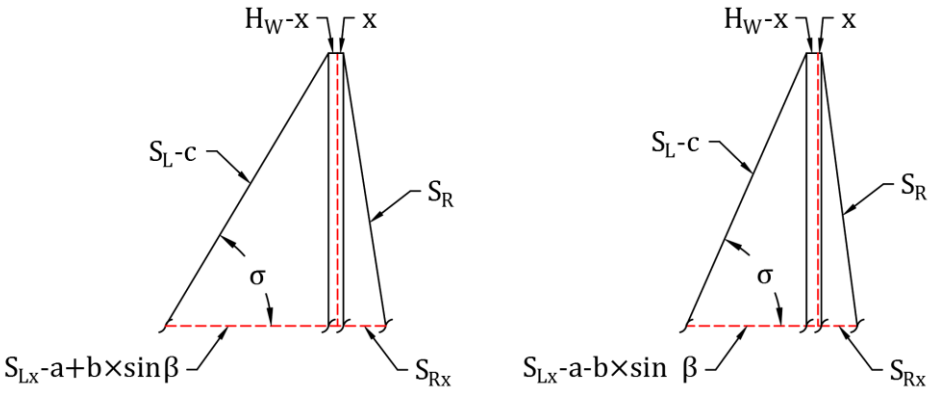

Fig. 9. Upper part of 2D drawings shown in Fig. 8

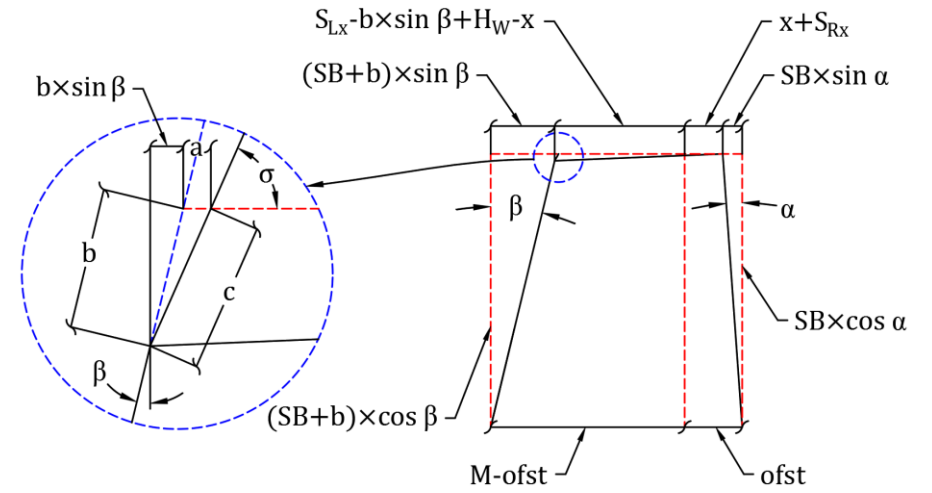

Fig. 10. Lower part of 2D drawings shown in Fig. 8

In the first step, using Eq. (1)-(2) (see Fig. 10) and Eq. (3) (see Fig. 8), the values of α, β, and b, which are the only unknown parameters of these equations, are calculated.

$$ofst \Big/ (S_B \sin\alpha) = (M - ofst) \Big/ ((S_B + b) \sin\beta) \quad (1)$$

$$S_B \cos\alpha = (S_B + b) \cos\beta \quad (2)$$

$$SB_L{}^2 - (\pm S_B \sin\beta + M \pm S_B \sin\alpha)^2 - (S_B \cos\alpha - S_B \cos\beta)^2 = 0 \quad (3)$$

By solving Eq. (1) and Eq. (2) for α, the value of β and b can be determined according to α satisfying Eq. (4) and Eq. (5).

$$\beta = \tan^{-1}\left((M - ofst)\tan\alpha \Big/ ofst\right) \quad (4)$$

$$b = \frac{ofst \times S_B \cos\alpha \cot\alpha}{\sqrt{(M - ofst)^2 + ofst^2 \cot^2\alpha}} + \frac{(M - ofst)^2 S_B \sin\alpha}{ofst\sqrt{(M - ofst)^2 + ofst^2 \cot^2\alpha}} - S_B \quad (5)$$

The value of α is increased iteratively from zero and the value of β and b is determined by Eq. (4) and Eq. (5) accordingly. The algorithm computes the value of unknown parameters with the accuracy of two decimal places. In order to decrease the number of iterations, α is initially increased with one-degree interval and when the sign of Eq. (3) is changed, the interval is divided by ten. This process continues until Eq. (3) is satisfied.

In the second step, based on the same approach, the values of the rest of unknown parameters are also determined. In this respect, the value of x is decreased iteratively from $H_W/2$ (the maximum possible value for x), and S_{Rx}, S_{Lx}, a, SB_{Lx}, c, σ, S_L are determined sequentially satisfying Eq. (6)-(10) (see Fig. 10); Eq. (11)-(12) (see Fig. 9), and Eq. (13) (see Fig. 8). The solution is achieved when Eq. (13) is satisfied.

$$x + S_{Rx} = ofst \pm S_B \sin\alpha \tag{6}$$

$$ofst \Big/ (x + S_{Rx}) = (M - ofst) \Big/ (S_{Lx} \pm b \sin\beta + H_W - x) \tag{7}$$

$$x \Big/ S_{Rx} = (H_W - x) \Big/ (S_{Lx} - a \pm b \sin\beta) \tag{8}$$

$$c^2 = a^2 + b^2 \mp 2\, a\, b \sin\beta \tag{9}$$

$$\tan\sigma = b \cos\beta \Big/ a \mp b \sin\beta \tag{10}$$

$$S_R{}^2 - S_{Rx}{}^2 = (S_L - c)^2 - (S_{Lx} - a \pm b \sin\beta)^2 \tag{11}$$

$$(S_L - c) \cos\sigma = S_{Lx} - a \pm b \sin\beta \tag{12}$$

$$SB_{Lx} = S_{Lx} + H_w + S_{Rx} \tag{13}$$

Based on the identified parameters, the sling angles, θ_L and θ_R (the angle of the slings above the spreader bar), and *RAI* are computed efficiently by Eq. (14) and Eq. (15), respectively.

$$\begin{aligned} \theta_L &= \sigma - \cos^{-1}\left(\frac{SB_L}{SB_{Lx}}\right) \\ \theta_R &= \cos^{-1}\left(\frac{S_{Rx}}{S_R}\right) + \cos^{-1}\left(\frac{SB_L}{SB_{Lx}}\right) \end{aligned} \tag{14}$$

$$RAI = S_L - S_R \tag{15}$$

The procedures of the proposed algorithm described above are operated repetitively to calculate the sling angles and RAI since the designer module frequently needs the results of Task1 in the solver module in order to design rigging components from bottom level to top level in the rigging assemblies. At this junction, it should be noted that the solver module removes Eq. (8)

when it calculates the sling angles and RAI at the second level of the rigging assembly since there is no hook component at this level. As a result, the values of H_W and x are set as zero at the second level. In this respect, the values of other unknown parameters (S_{Rx}, S_{Lx}, a, SB_{Lx}, c, σ, S_L) are determined using Eq. (6), Eq. (7) and Eq. (9)-(13).

3.3.2 Task 2

When the COG is offset, in order to balance the load, sling length adjustment is implemented by mounting a chain of shackles on one of the two slings above the spreader bar depending on the direction of the COG offset due to identical slings in length. The chain of shackle is used to increase the length of sling with a specific amount *RAI* to take up the slack between the sling end and the shackle attached to the spreader bar (see Fig. 6). At this junction, it should be noted that each shackle has a specific inside length which can take up a specific amount of slack. In this respect, the total inside length of the shackles that are used in the chain of shackles must be as close as possible to the *RAI*. In this respect, the objective function is defined as follows.

$$f = \text{MIN}\left|\text{RAI} - \sum_{i=1}^{N} n_i C_i\right| \tag{16}$$

Where:

- f: is the minimum absolute difference between the required amount of increase and the total length made by the chain of shackle.
- *RAI*: the Required Amount of Increase
- N: total number of shackles available with different size
- n_i: number of i shackles used in the chain

- C_i: inside length of i shackle.

Needless to say that the feasible shackles mounted to the sling must meet the minimum required capacity of the sling. That is, before selecting the shackles from the database, they are filtered based on the required capacity.

3.4 Designer Module

The designer module selects rigging components from the database to design the rigging assembly satisfied the required capacity of each rigging component. The selection of the rigging component process is implemented from the lowest to the highest level of the rigging assembly based on the module information and the sling angles which are already computed in the solver module. In this section, the design sequences of 4-point pick and 2-point pick segments of rigging assemblies are described since traditional rigging assembly of modules with N lifting points (4 to 16 lifting points depending on the module length) are designed based on the combination of these two segments. At the end of this section, the process of rigging component selection from the database and interaction between the database and the designer module is described.

3.4.1 Preliminary Design

The design of 4-point pick segments starts with designing a preliminary rigging assembly. In order to determine the sling angles using the system of equations mentioned in the solver module, the value of the known parameters (H_W, M, $ofst$, SB_L, S_R, and S_B) are required to be determined by the designer module. The first three parameters (H_W, M, and $ofst$) are the inputs of the system which are determined by the user. The initial value of the other three parameters (SB_L, S_R, and S_B) are determined based on a preliminary rigging assembly in which the COG is assumed to be in the middle of the 4 lifting points.

As the main objective of designing the preliminary rigging assembly is to provide the initial value of SB_L, S_R, and S_B, the required capacity of the rigging components in the preliminary design is not calculated precisely. Instead, the rigging components are selected from the database based on a roughly estimation of their required capacity. With that being said, the required capacity of

the shackles used at the lifting points and drop slings are considered as the average of W_1 to W_4 which are the weight forces applied to the lifting points obtained from the module's weight report (Fig. 11) . Based on this capacity, the shackles at the lifting points and drop slings are selected from the database and the value of S_B for the calculations at the second level, which is represented as $(S_B)_2$ in Fig. 11 is determined.

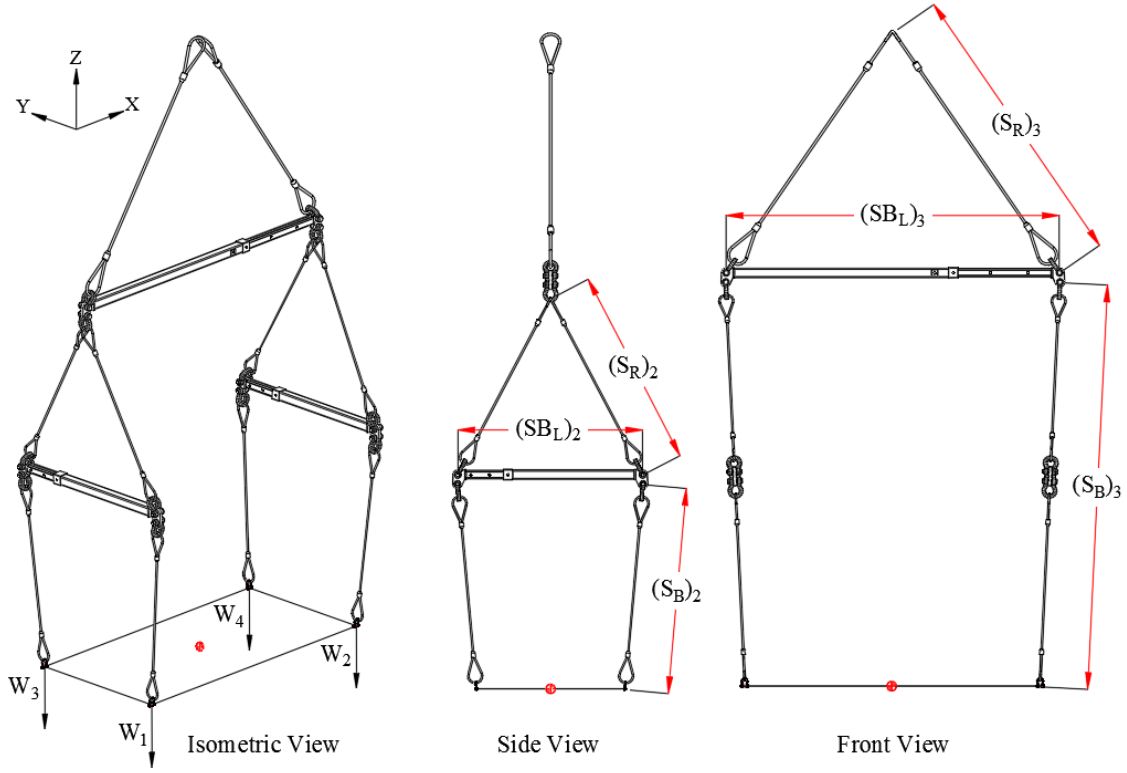

Fig. 11. Preliminary rigging assembly

The required capacity of the spreader bars at level two is considered as $(W_1 + W_2 + W_3 + W_4)/2$. Therefore, based on this capacity a spreader bar which has the closest length to the width of the module is selected from the database and the value of $(SB_L)_2$ is determined. As the capacity of a spreader bar is a function of its length and the length of slings which are used above it (this will be discussed with more details in the following sections), the value of $(S_R)_2$ is identified based on the selected spreader bar. Similarly, considering that the required capacity of the spreader bar

at level three is the summation of W_1 to W_4, the value of $(SB_L)_3$ and $(S_R)_3$ is determined.

3.4.2 4-Point Pick Segments

The sequences of designing 4-point pick segments can be described using the flowchart represented in Fig. 12. Once the suitable rigging components are selected from the database for the preliminary rigging assembly, the initial values of SB_L, S_R, and S_B are identified. In the next step, the solver (task 1) is called to calculate the sling angles at the first level of the rigging assembly. Since the angles of drop slings (α and β) should be closed to zero to satisfy one of design criteria, which the drop slings are perpendicular to the module, the lengths of the drop slings are increased when the difference between the length of the spreader bar and the distance between the end of lifting points is existed. However, in the practical view, it is difficult to establish the perpendicular between the drop slings and module. To overcome this practical limitation, this thesis uses the minimum acceptable angles of drop slings defined by the user. Based on this constraint, the lengths of the drop slings are increased by 5 ft. (length interval of the slings in the database) until the angles of the drop slings become smaller than the minimum acceptable angles. At this junction, it should be noted that the solver and designer modules are communicated interactively and frequently to update these sling angles when the lengths of the drop slings are changed.

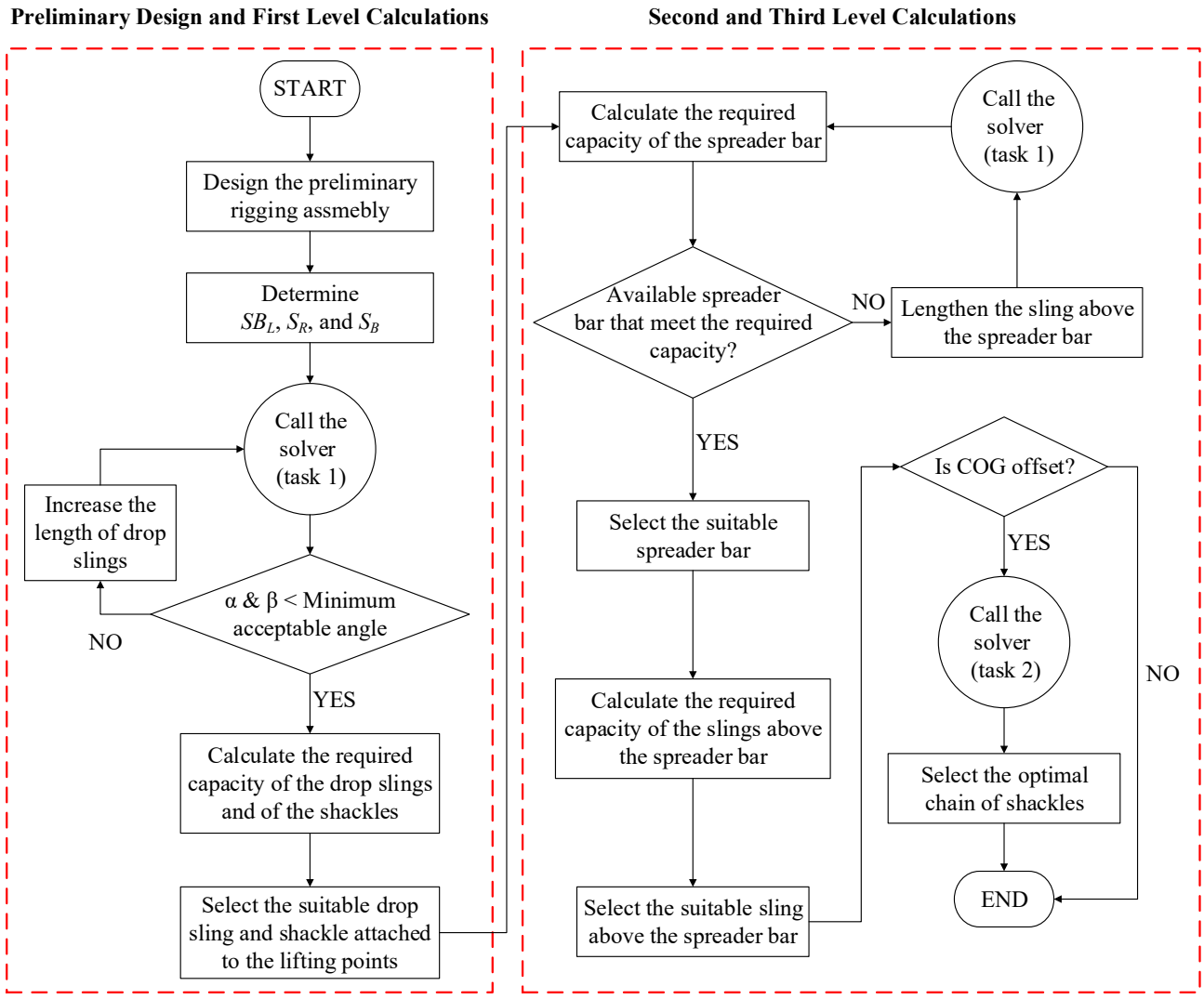

Fig. 12. 4-point pick segments designing procedure

In the next step, the required capacity of the drop slings and of the shackles mounted to the lifting points are calculated by analysing the free body diagram of the module as shown in Fig. 13. The forces equilibrium equation for the module in X and Y direction can be expressed as Eq. (17) and Eq. (18) respectively:

$$-F_{L1}\,sin\,\beta + F_{R1}\,sin\,\alpha = 0 \tag{17}$$

$$F_{L1}\,cos\,\beta + F_{R1}\,cos\,\alpha - W_L\,sec\,\delta - W_R\,sec\,\delta = 0 \tag{18}$$

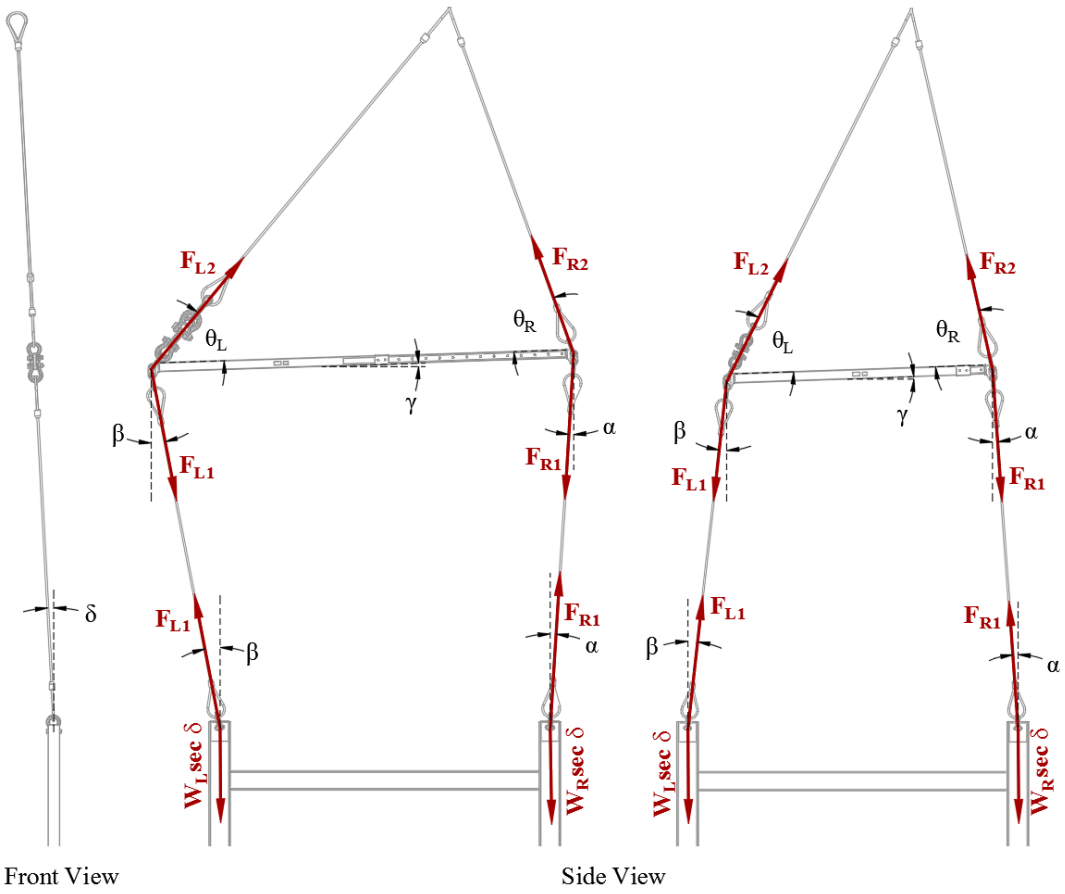

Fig. 13. Forces applied to the module and the rigging assembly

Therefore, the value of F_{L1} and F_{R1} is determined satisfying Eq. (19).

$$F_{L1} = (W_L + W_R)\ sec\ \delta\ csc(\alpha + \beta)\ sin\ \alpha$$
$$F_{R1} = (W_L + W_R)\ sec\ \delta\ csc(\alpha + \beta)\ sin\ \beta \quad (19)$$

Where:

- F_{L1} and F_{R1} are the sling forces.
- α and β are the sling angles.
- W_L and W_R are the weight forces applied to the lifting points which are obtained from the module's weight report.

- δ is the angle of plane which contains the slings and the spreader bar at the second level with the vertical plane which is determined by the solver (task 1). δ is, in fact, equal to either α or β where the sling angles are calculated at the third level of the rigging assembly (see Fig. 8).

The maximum of F_{L1} and F_{R1} is the required capacity of the drop slings and of the shackles. This required capacity is used for all of the drop slings and shackles at the first level of rigging assembly which results in a conservative design approach. This approach is used for the entire rigging assembly. Meaning that, at each level of the rigging assembly, the required capacity of the rigging components is determined based on the maximum required capacity at that level and an identical rigging component (e.g. spreader bar, sling, shackle etc.) is used for the entire level. Of course, the overall weight of the rigging assembly is increased as a consequence of a conservative design approach, however, this increase in weight is not considerable compared to the overall lifting load (the weight of the rigging assembly plus the weight of module). On the other hand, using identical rigging components at each level of the rigging assembly has the benefit of simplicity and consistency which prevents confusion for the riggers at the jobsite.

Next, the suitable spreader bar for the second level is selected based on its required capacity which is: $(W_L + W_R)\ sec\ \delta$ .In selecting spreader bars, it should be noted that, as shown in Table 1, the rated capacity of a spreader bar is getting increased when the length of slings is also increased. By increasing the length of slings, the angle between the slings and the spreader bar is increased which in turn decreases the bending moment applied to the spreader bar. Based on this fact, when there is not any available spreader bar in the database that meets the required capacity, the lengths of the slings are increased to obtain the higher capacity of the spread bar. In this case, of course,

the solver module is called to recalculate the angles between the slings and the spreader bar.

Table 1. Capacity chart of a spreader bar (lbs.)
(Table source: NCSG Engineering Ltd. capacity charts)

Sling Length (ft.)	Spreader bar length (ft.)					
	8	9	10	11	12	13
10	31,000	30,000	29,400	28,400	26,400	14,000
15	32,800	32,400	32,000	31,600	31,200	24,000
20	33,200	33,000	32,800	32,600	32,400	30,000
25				33,000	33,000	32,800
30						33,000

In the next step, the required capacity of the slings at the second level is calculated which is the maximum sling forces at this level. The forces equilibrium equation for the spreader bar in X and Y direction (see Fig. 13) can be expressed as Eq. (20) and Eq. (21) respectively:

$$F_{L2}\cos(\theta_L+\gamma)-F_{R2}\cos(\theta_R-\gamma)+F_{L1}\sin\beta-F_{R1}\sin\alpha=0 \tag{20}$$

$$F_{L2}\sin(\theta_L+\gamma)+F_{R2}\sin(\theta_R-\gamma)-F_{L1}\cos\beta-F_{R1}\cos\alpha=0 \tag{21}$$

By replacing F_{L1} and F_{R1} from Eq. (19) the value of F_{L2} and F_{R2} can be determined satisfying Eq. (22) as follows:

$$\begin{aligned} F_{L2} &= (W_L+W_R)\sec\delta\cos(\theta_R-\gamma)\csc(\theta_L+\theta_R) \\ F_{R2} &= (W_L+W_R)\sec\delta\cos(\theta_R+\gamma)\csc(\theta_L+\theta_R) \end{aligned} \tag{22}$$

Where:

- θ_L and θ_R are the sling angles above the spreader bar.
- γ is the slope of the spreader bar.

The maximum value of F_{L2} and F_{R2} is considered as the required capacity of the slings at level two

and based on that the suitable slings at the second level are selected from the database. With the same procedures as those used to select the spreader bar and slings at the second level of the rigging assembly, the selection of spread bar and slings at the third level of the rigging assembly is implemented.

Finally, after selecting the suitable spreader bars and slings at all levels of the rigging assembly, if the COG is offset from the COM, the solver (task 2) is called to select the optimal chain of shackles mounted to the slings.

3.4.3 2-Point Pick Segments

As mentioned earlier, 2-point pick segments are used either inside of the 4-point pick segments or in the middle of the whole rigging assembly (see Fig. 5). According to the required length on the bottom of the drop slings, the height of this segment is adjusted using the turnbuckles (see Fig. 7). In this context, the algorithm of designing 2-point pick segments is described using the flowchart represented in Fig. 14. The algorithm starts with calculating the desired total height of the segment ($H_{Desired}$) which must be equal to the height of the 4-point pick segment or the height of the entire rigging assembly depending on the location of 2-point pick segment. In this respect, the lengths of drop slings (SL_{1st}) are the same as the lengths of those used in the 4-point pick segments. The initial sling length at the second level (SL_{2nd}) is also set by the length of those used at the second level of the 4-point pick segments and the initial sling length at the third level (SL_{3rd}) is set to the shortest lengths of slings which are available in the database ($\text{Min}(SL_{DB})$). The solver module (task 1) is then called to calculate the sling angles and based on the lengths and angles of slings, the height of the 2-point pick segment excluding the height of the turnbuckles (H_{Slings}) is calculated. The difference between H_{Slings} and $H_{Desired}$ which referred to as remaining height

(H_{Remain}) must be taken up by the turnbuckles. H_{Remain} is determined satisfying Eq. (23).

$$H_{Remain} = H_{Desired} - H_{Slings} = H_{Desired} - (H_{SL_{1st}} + H_{SL_{2nd}} + H_{SL_{3rd}}) \quad (23)$$

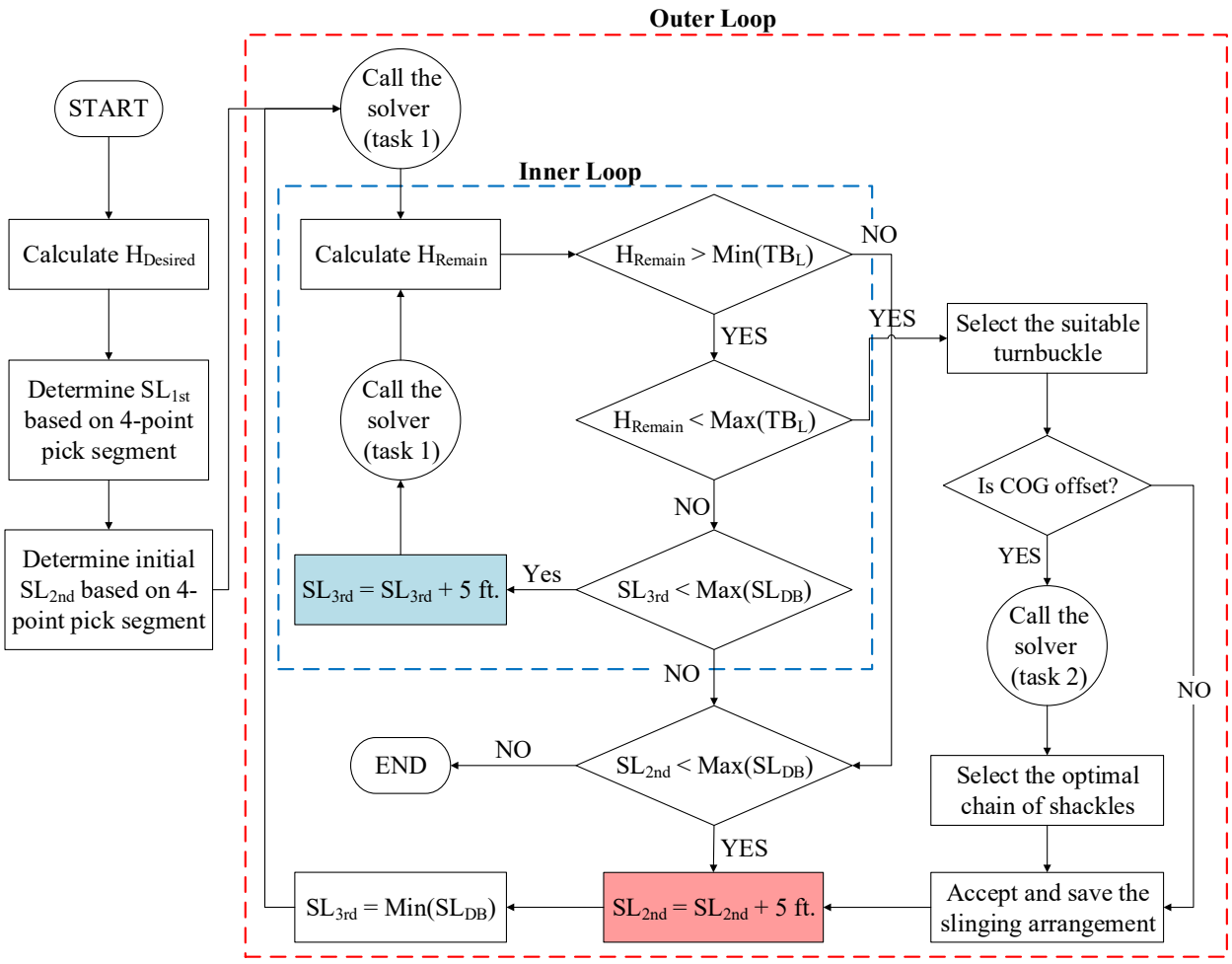

Fig. 14. 2-point pick segments designing procedure

When H_{Remain} is between the minimum and maximum opening length of the available turnbuckles ($Min(TB_L)$ and $Max(TB_L)$) in the database, the first feasible slinging arrangement is generated. Otherwise, SL_{2nd} and SL_{3rd} are increased by 5 ft. (length interval of the slings in the database) in a nested loop (loop within a loop) until the H_{Remain} is more than the $Min(TB_L)$ and less than $Max(TB_L)$ in order to generate all of the feasible sling arrangements. In the outer loop SL_{2nd}

is increase by 5 ft. from its initial length to the longest sling available in the database ($Max(SL_{DB})$). Similarly, in the inner loop SL_{3rd} is increase by 5 ft. from its initial length to $Max(SL_{DB})$. It this way all the sling length combinations are generated and for each combination the suitable turnbuckle (if there is any) is selected. The algorithm is terminated when SL_{2nd} exceeds $Max(SL_{DB})$. It should be noted that for the accepted configurations, if the COG is offset from the COM in Y-axis, the solver module (task 2) is called to select the optimal chain of shackles attached to one of the two slings above the spreader bar.

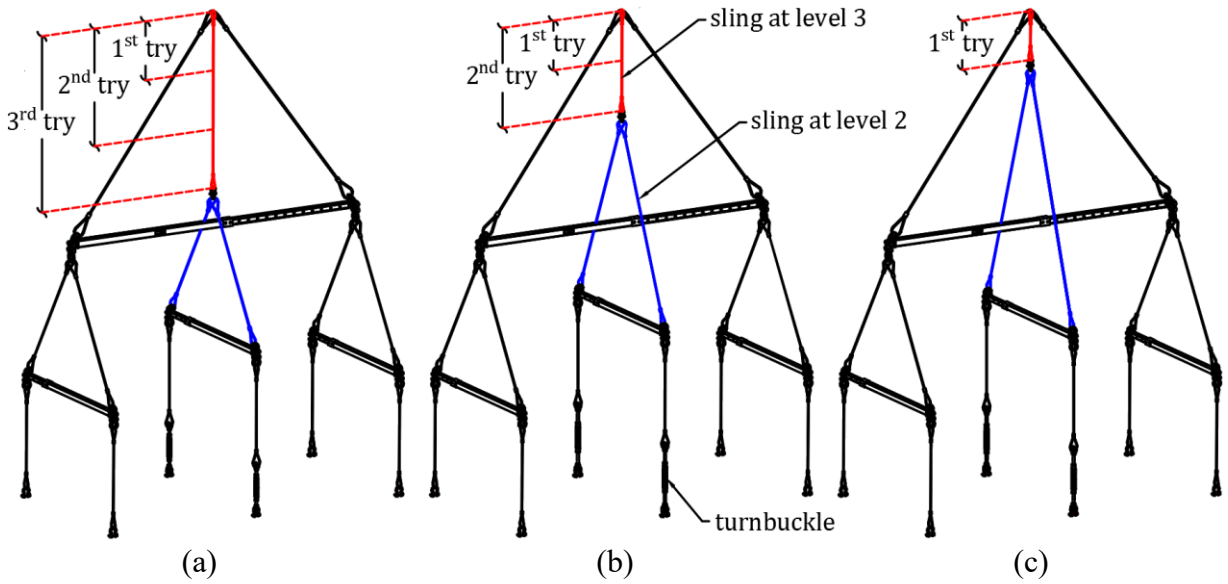

Fig. 15. Feasible slinging arrangements of a 2-point pick segment

In order to provide a better understanding of the algorithm, Fig. 15 shows three feasible slinging arrangements of a 2-point pick segment located inside of a 4-point pick segment. In all of the three slinging arrangements, the drop slings are identical in length and are the same as those used in the 4-point pick segments. In Fig. 15(a), the slings at level 2 (blue slings) has the same length as those used in the second level of 4-point pick segment (i.e. the initial value of sling length

at the second level); and the initial sling length at level 3 (the length shown as 1st try) is set to $Min(SL_{DB})$. In this case, there is no available turnbuckle since H_{Remain} is more than Max(TB_L). Therefore, the sling length at level 3 is increased continuously (2nd try and 3rd try) until the H_{Remain} is between the $Min(TB_L)$ and $Max(TB_L)$. In the next loop round (Fig. 15(b)) the sling length at the second level is increased by 5 ft. and the length of sling at the third level is increased continuously from its initial value (the length shown as 1st try) until H_{Remain} is between the $Min(TB_L)$ and $Max(TB_L)$. With the same process, the third feasible slinging arrangement is generated (Fig. 15(c)).

3.4.4 Selecting Rigging Components From The Database

In order to select the rigging components, within the deign process of the rigging assembly, the required data is interactively transferred from designer module (Microsoft Visual C#.NET) to the database (Microsoft Excel), and vice versa. The selection process of rigging components slightly varies based on different rigging types (spreader bars, slings, etc.). This process is explained for each of the rigging components that are used in the rigging assembly.

3.4.4.1 Shackles

Except from the shackles that are mounted on the spreader bars (4 shackles on each spreader bar), shackles are implemented in the in rigging assemblies at three different locations:

I. shackles that are attached to the lifting points.

II. The chain of shackles that are mounted above the spreader bars to balance the module in the cases that COG is offset from the module's center (see Fig. 6).

III. The chain of shackles used in the 2-point pick segments to connect the slings which are located at the second level of to the sling at the third level. (see Fig. 7).

The system might select shackles that are not compatible in size with each other or lifting

points (lugs). Therefore, in order to have better control on the selection of shackles at different locations of the rigging assembly, three columns named “Availability”, are defined in the database (Fig. 16). The value of the cells under these three columns can be either “Yes” or “No”. The system only selects from the available shackles. With this feature, the user can modify the availability of the shackles and rerun the system once an incompatibility in the size of shackles is encountered in the 3D model.

Input	
Required capacity (ton)	23.80

Output				
Working Load Limit (t)	Weight (lbs)	C (in)	B (in)	dwg File path
25.00	33.91	7.00	2.04	c:/Rigging (

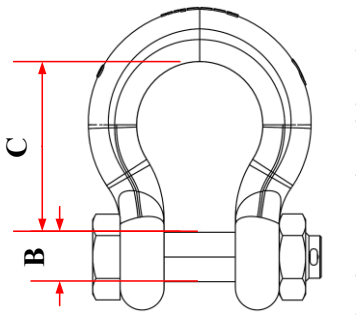

Working Load Limit (t)	Weight (lbs)	C (in)	B (in)	dwg File path	Availability (1)	Availability (2)	Availability (3)
150.00	338.00	14.50	4.26	c:/Rigging (	No	No	No
120.00	265.00	14.83	3.30	c:/Rigging (	No	No	No
85.00	154.00	13.00	3.24	c:/Rigging (	No	No	Yes
55.00	98.25	10.50	2.74	c:/Rigging (	Yes	Yes	Yes
35.00	52.25	7.75	2.25	c:/Rigging (	Yes	No	Yes
25.00	33.91	7.00	2.04	c:/Rigging (	Yes	No	Yes
17.00	19.00	5.75	1.66	c:/Rigging (	Yes	No	No
13.50	15.83	5.25	1.53	c:/Rigging (	Yes	No	No
12.00	11.71	4.69	1.40	c:/Rigging (	Yes	No	No
9.50	8.27	4.25	1.25	c:/Rigging (	Yes	No	No
8.50	5.66	3.75	1.15	c:/Rigging (	No	No	No
6.50	3.95	3.31	1.02	c:/Rigging (	No	No	No
4.75	2.72	2.81	0.89	c:/Rigging (	No	No	No

Fig. 16. Shackle sheet in the Excel database

In order to select the suitable shackle from the database, the following steps are implemented in the system:

I. The designer module sends the required capacity to the input box which is located above the table in Fig. 16.

II. The table is filtered based on the available shackles that meet the required capacity.

III. The row of the table that has the minimum working load limit (capacity) is selected and copied to the output box above the table using index and match formula in Excel.

IV. Finally, the value of the parameters in the output box is sent back to the designer module.

3.4.4.2 Spreader bars

As it was mentioned earlier, the capacity of a spreader bar is a function of its length and the length of slings that are used above it (i.e. the angle of slings above it). By increasing the length of sling above the spreader bars (i.e. increasing the angle of sling above the spreader bar), higher capacity of the spreader bar can be gained. In this context the sequence of selecting the suitable spreader bar from the database is as follows:

I. The required capacity, the required spreader bar's length which is determined based on the distance between the lifting points, and the minimum angle of sling angles above the spreader bar (i.e. $Min(\theta_L, \theta_R)$ calculated by the solver module) are sent by the designer module to the input box which is located above the table in Fig. 17.

II. The "Bar length" column is filtered with the closest value to the required spreader bar's length.

III. The "Angle" column is filtered with values that are less than the angle entered in the input box.

IV. The unavailable spreader bars are filtered out using the “Availability column”.

V. The row of the table that has the minimum capacity is selected and copied to the output box above the table.

VI. Lastly, the value of the parameters in the output box is sent back to the designer module.

It should be noted that one of the output parameters in selecting the spreader bars is the corresponding sling length in the selected row which is used in selecting the suitable sling.

Input	
Required Bar Length (ft)	18.2
Required Capacity (lbs)	92,000
Angle	63.8

Output										
Bar length (ft)	Capacity (lbs)	Sling length (ft)	Angle	Shackles (t)	Weight (lbs)	C + B/2 (in)	Name	Height	Horizontal ofst (in)	dwg File path
18	93,600	25	69.5	25	790.64	8.75	NC6L 13-22	6	0.25	c:/Rigging (

Bar length (ft)	Capacity (lbs)	Sling length (ft)	Angle	Shackles (t)	Weight (lbs)	C + B/2 (in)	Name	Height	Horizontal ofst (in)	dwg File path	Availability
12	98,000	30	78.7	25	565.64	8.75	NC-6S 8-13	6	0.25	c:/Rigging (	No
10	98,000	25	78.8	25	565.64	8.75	NC-6S 8-13	6	0.25	c:/Rigging (	No
8	98,000	20	78.9	25	565.64	8.75	NC-6S 8-13	6	0.25	c:/Rigging (	No
22	97,600	50	77.5	25	790.64	8.75	NC6L 13-22	6	0.25	c:/Rigging (	Yes
17	97,600	40	78.0	25	790.64	8.75	NC6L 13-22	6	0.25	c:/Rigging (	Yes
13	97,600	30	77.8	25	565.64	8.75	NC6L 13-22	6	0.25	c:/Rigging (	Yes
11	97,600	25	77.7	25	790.64	8.75	NC-6S 8-13	6	0.25	c:/Rigging (	No
18	97,400	40	77.2	25	565.64	8.75	NC6L 13-22	6	0.25	c:/Rigging (	Yes
16	97,400	35	77.1	25	790.64	8.75	NC6L 13-22	6	0.25	c:/Rigging (	Yes
9	97,400	20	77.5	25	565.64	8.75	NC-6S 8-13	6	0.25	c:/Rigging (	No
19	97,200	40	76.5	25	565.64	8.75	NC6L 13-22	6	0.25	c:/Rigging (	Yes
12	97,200	25	76.5	25	790.64	8.75	NC-6S 8-13	6	0.25	c:/Rigging (	No
22	97,000	45	76.1	25	565.64	8.75	NC6L 13-22	6	0.25	c:/Rigging (	Yes
10	97,000	20	76.0	25	790.64	8.75	NC-6S 8-13	6	0.25	c:/Rigging (	No
15	96,800	30	75.9	25	790.64	8.75	NC6L 13-22	6	0.25	c:/Rigging (	Yes
18	96,600	35	75.4	25	790.64	8.75	NC6L 13-22	6	0.25	c:/Rigging (	Yes
22	[illegible]	[illegible]	[illegible]	25	565.64	8.75	NC6L 13-22	6	0.25	c:/Rigging (	Yes

Fig. 17. Spreader bar sheet in the Excel database

3.4.4.3 Slings

Selecting slings from the database is quite straightforward. The following steps are required in a sequence in order to select the slings:

Input	
Required Length (ft)	30
Required Capacity (lbs)	53,281

Output				
Diameter (in)	Length (ft)	Capacity (lbs)	Weight (lbs)	dwg File path
1.75	30	56,000	237.33	c:/Rigging

Diameter (in)	Length (ft)	Capacity (lbs)	Weight (lbs)	dwg File path	Availability
4	20	260,000	1,203.60	c:/Rigging	Yes
4	25	260,000	1,351.60	c:/Rigging	Yes
4	30	260,000	1,499.60	c:/Rigging	Yes
4	35	260,000	1,647.60	c:/Rigging	Yes
4	40	260,000	1,795.60	c:/Rigging	Yes
3.5	20	204,000	898.65	c:/Rigging	No
3.5	25	204,000	1,012.15	c:/Rigging	No
3.5	30	204,000	1,125.65	c:/Rigging	No
3.5	35	204,000	1,239.15	c:/Rigging	No
3.5	40	204,000	1,352.65	c:/Rigging	No
3	15	154,000	556.80	c:/Rigging	Yes

Fig. 18. Sling sheet in the excel database

I. The required capacity and length are sent by the designer module to the input box which is located above the table in Fig. 18.

II. The table is filtered based on the slings that are available and meet the required capacity.

III. The row of the table that has the minimum capacity is selected and copied to the output box above the table.

IV. The value of the parameters in the output box is sent back to the designer module.

3.4.4.4 Turnbuckles

The turnbuckles are attached to the drop slings of the 2-point pick segments in order to adjust the height of this segment. The turnbuckles are selected from the database based on their capacity and minimum and maximum opening length. The selection process of turnbuckles includes:

Input	
Required Opening Length (in)	40.06
Required Capacity (lbs)	20,189

Output					
Name	Weight (lbs.)	Max. opening length (in)	Min. opening length (in)	Working Load Limit (lbs)	dwg File path
1-1/2 x 24	20.70	61.02	38.58	21,407	c:/Riggin

Name	Weight (lbs.)	Max. opening length (in)	Min. opening length (in)	Working Load Limit (lbs)	dwg File path	Availability
2-3/4 x 24	98.00	73.94	51.38	74,957	c:/Riggin	Yes
2-1/2 x 24	88.00	72.05	49.37	59,966	c:/Riggin	Yes
2 x 24	45.40	65.83	45.31	37,038	c:/Riggin	Yes
1-3/4 x 18	25.00	51.57	36.73	27,999	c:/Riggin	Yes
1-3/4 x 24	28.70	63.54	42.68	27,999	c:/Riggin	No
1-1/2 x 12	16.90	37.05	26.57	21,407	c:/Riggin	Yes
1-1/2 x 18	19.30	48.98	32.48	21,407	c:/Riggin	No
1-1/2 x 24	20.70	61.02	38.58	21,407	c:/Riggin	Yes
1-1/4 x 12	11.90	36.06	25.23	15,212	c:/Riggin	Yes
1-1/4 x 18	13.60	47.95	31.22	15,212	c:/Riggin	Yes
1-1/4 x 24	14.20	60.55	37.83	15,212	c:/Riggin	Yes

Fig. 19. Turnbuckle sheet in the excel database

I. The required capacity and required opening length of the turnbuckle is sent to the input box which is located above the table in Fig. 19.

II. The “Min. opening length” column of the table is filtered with the values that are less than the required opening length.

III. The “Max. opening length” column of the table is filtered with the values that are

greater than the required opening length.

IV. The unavailable turnbuckles are filtered out using the “Availability” column of the table.

V. Among the remaining rows of the table, the one that has the minimum capacity is selected and copied to the output box above the table.

VI. The value of the parameters in the output box is sent back to the designer module.

3.5 3D Visualizer Module

The 3D visualizer is developed using an AutoCAD programming interface (API) written in C# language within the .Net framework. The code uses a nested structure to create a 3D model of the designed rigging assembly. All of the selected rigging components in the rigging assembly designer are stored in the database as AutoCAD 3D blocks and are inserted one by one into the model space and positioned in their suitable coordinates through a sequence of AutoCAD commands such as copy, move, rotate, etc. The inserted blocks need to be manipulated in order to correspond to the results of the rigging assembly designer (i.e., length and angle of rigging components). For instance, the manipulation process for spreader bars, which are equipped with 4 shackles as a 3D block (Fig. 20), includes exploding the block, selecting each of the shackles and rotating them, selecting the whole block, and moving it to the suitable position. The required parameters in performing these tasks are collected from both the database and the results of the rigging analyses. For the spreader bar shown in Fig. 20, α, β, θ_L, and θ_R are variable parameters that are assigned by the results of the solver and designer, while H and SB_L are constant values obtained from the database-stored parameters of the block. These parameters are collected and used as the inputs of the AutoCAD commands. Fig. 20(a) shows the original configuration of the block, and Fig. 20(b) shows the manipulated block.

In order to have better control in terms of selecting the rigging components, they are differentiated with different colors and layers. Thus, the rigging components can be selected using a selection filter based on the color and the layer that has been assigned to them. Moreover, to reduce some of the repetitive tasks required in manipulating the inserted blocks, dynamic blocks, which are designed parametrically and can be modified using their dynamic parameters, are implemented. For instance, instead of selecting and then rotating a rigging component to a specific

angle, a dynamic parameter in conjunction with a rotate action is defined to perform these two tasks by only assigning an angle to that parameter. Consequently, the parameters of the blocks are better controlled and the overall execution time of the code is reduced.

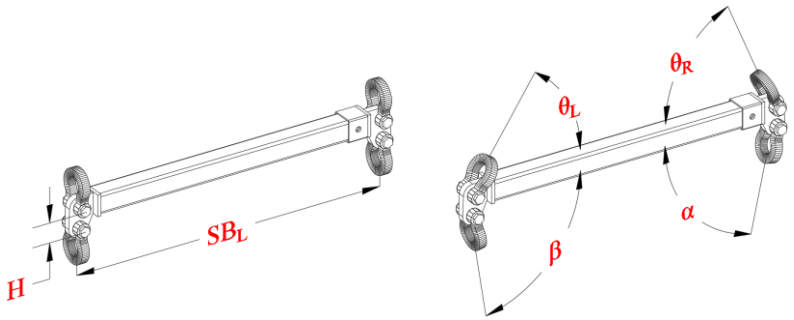

(a) (b)

Fig. 20. Constant and variable parameters of a spreader bar block

Chapter 4: Case Studies

In order to verify and validate the proposed methodology, the rigging assembly design of two different modules are used as the case studies. The selected modules are a 6-point pick and a 4-point pick modules. The rigging assembly design and visualization process of these modules could typically take 1.5 hour in total for an experienced lift engineer. Whereas, using the proposed methodology, it takes about 10 minutes to accomplish the same series of tasks (including the potential required manual modifications) with higher accuracy.

A significant amount of time can be saved for each lift study in the planning phase of multi-heavy lift projects. The methodology has been tested on 50 different modules and no design errors were encountered. On the other hand, manual designs may involve human errors that lead to reworks and wasted time, and most importantly may involve safety issues regarding failure of the rigging components.

4.1 Case Study 1

The first module which is used as case study is an 88,000 lb (39.9 tonne) module that has six lifting points. The width and length of the module is 376 in (9.55 m) and 209 in (5.31 m), respectively. The COG is offset from the bottom left corner of the module (P1) by 220 in (5.58 m) and 84 in (2.13 m) in X and Y directions, respectively. The width of the hook and maximum acceptable angle of drop slings as input are defined as 17 in (0.43 m) and 3°, respectively, through the dialogue box shown in Fig. 21. After pressing the “Rigging Analysis” button based on the available rigging components stored in the Excel database, potential rigging assembly design alternatives are listed in the “Report” text box located on the right side of the interface. The user can then create a 3D model for one of the alternatives by pressing the “3D visualization” button.

The sequence of design procedures for the rigging assembly, based on the input parameters, is described in this section.

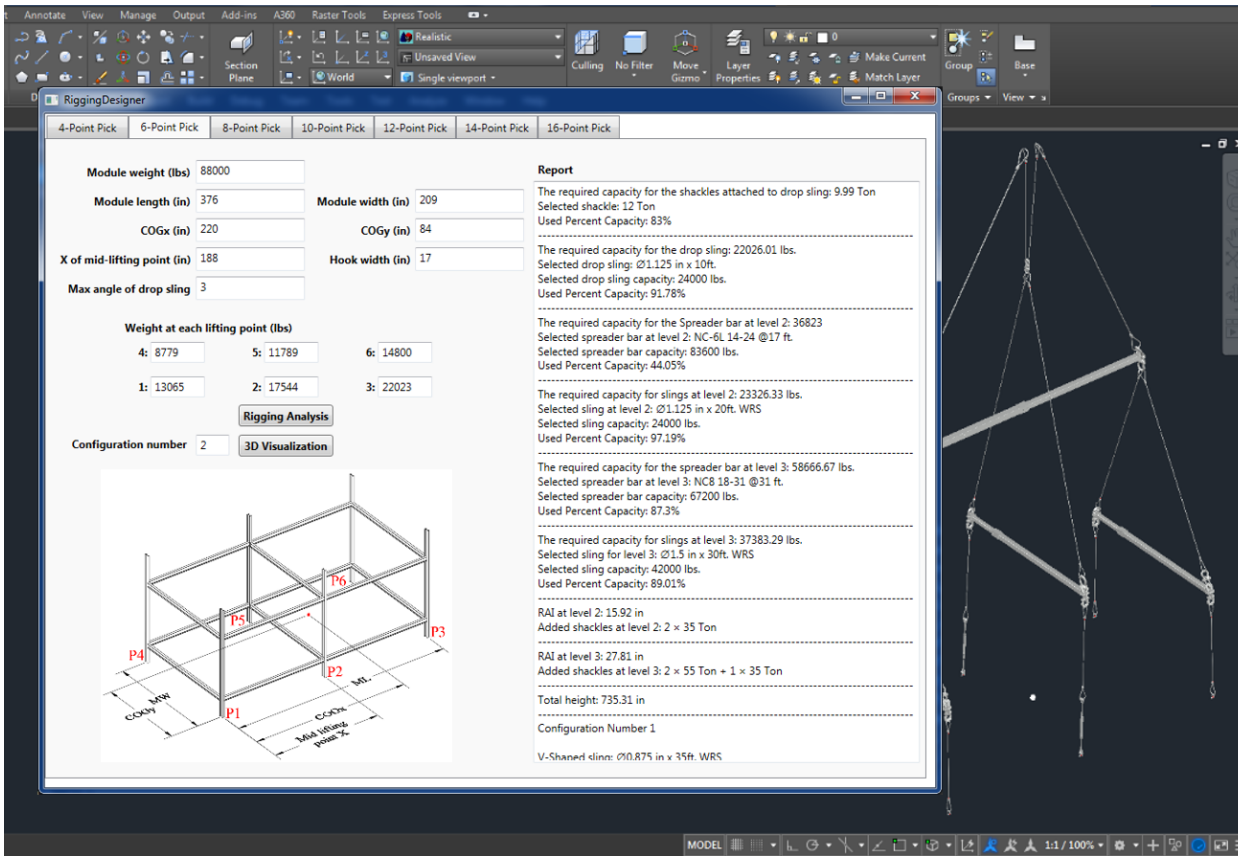

Fig. 21. The user interface of the proposed methodology

The design of the 4-point pick segment of the rigging assembly begins with designing a preliminary rigging assembly which is performed by the designer module to provide the initial values of the known parameters required in task 1 of the solver module. Assuming that the COG is in the COM, a symmetrical rigging assembly is designed. Table 2 shows the selected rigging components in the preliminary design.

Table 2. Selected rigging components for the preliminary rigging assembly

Rigging component	Description
Shackle at the lifting points	8.5-tonne (inside length = 3.75 in)
Sling length at the first level (drop sling)	10 ft.
Sling length at the second level	15 ft.
Sling length at the third level	25 ft.
Spreader bar length at the second level	17 ft.
Spreader bar length at the third level	31 ft.

The sling angles at the first and second levels of the rigging assembly and the *RAI* are calculated in a two-dimensional plane containing the spreader bar at the second level and the two slings above it (represented as the red plane in Fig. 22). By measuring S_R, SB_L, and S_B on the preliminary rigging assembly and collecting *M* and *ofst* from the inputs of the system, the known parameters are determined: S_R = 188 in (4.79 m), SB_L = 204 in (5.18 m), S_B = 133 in (3.38 m), *M* = 209 in (5.31 m), and *ofst* = 84 in (2.13 m). It should be noted that H_W is set to zero for the calculations at the first and second levels.

Task 1 of the solver is called and the values of sling angles are computed as $\alpha = 0.87°$, $\beta = 1.29°$, $\theta_L = 54.33°$, and $\theta_R = 64.29°$. As the drop sling angles (α and β) are smaller than the maximum acceptable angle (3°) defined by the user, it is not necessary to increase the lengths of drop slings. The required capacity of the drop slings and the shackles attached to them is calculated using the designer module as 22,026 lb (9.99 tonne). Then, the suitable drop slings (Ø1-1/8 in. × 10 ft) and shackles, which have a capacity of 12 tonne, are selected from the database. The required capacity of the spreader bar at the second level is 36,823 lb (16.7 tonne). However, based on considering the selected sling length (15 ft) at the second level in the preliminary design, there is

not a spreader bar available that can meet the required capacity. Therefore, the length of the sling at the second level is increased to the next longer sling in the database (20 ft) and the value of S_R is updated to 249 in (6.32 m). Task 1 of the solver is called to recalculate the sling angles. With the updated sling angles ($\theta_L = 62.54°$, $\theta_R = 70.76°$), the spreader bar with the length of 204 in (5.18 m) and capacity of 83,600 lb (37.92 tonne) is selected because it satisfies the required capacity. Based on the required capacity of the slings at level 2, which is 23,326 (10.58 tonne), the suitable sling (i.e. Ø1-1/8 in × 20 ft) with the capacity of 24,000 lb (10.89 tonne) is selected.

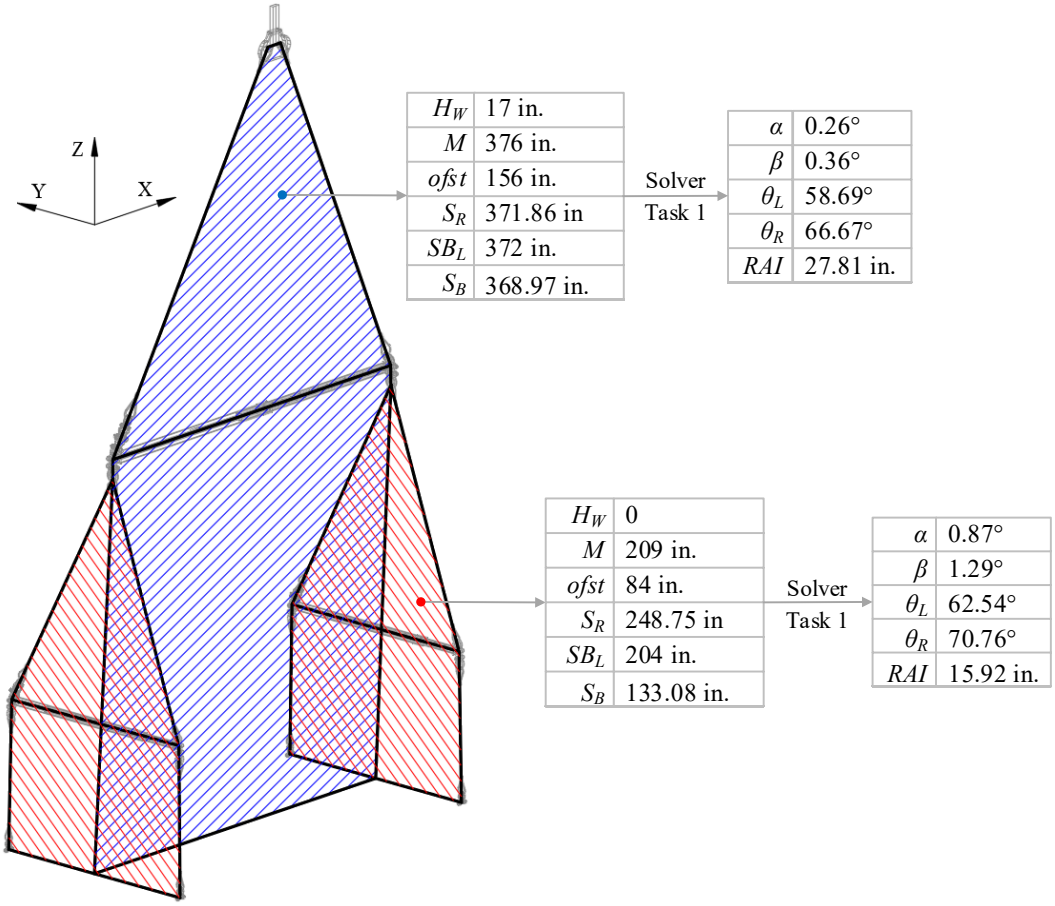

Fig. 22. Calculations of sling angles and *RAI* in two-dimensional planes

The sling angles at the third level of the rigging assembly and the *RAI* are calculated in a

two-dimensional plane containing the spreader bar at the third level and the two slings above it (represented as the blue plane in Fig. 22). The known parameters required in Task 1 of the solver are determined to be H_W = 17 in (0.43 m), S_R = 312 in (7.92 m), SB_L = 372 in (9.45 m), S_B = 369 in (9.37 m), M = 376 in (9.55 m), and *ofst* = 156 in (3.96 m). Based on these inputs, the results of the solver are α = 0.26°, β = 0.36 °, θ_L = 52.92°, and θ_R = 61.82°. Considering the lengths and angles of slings above the spreader bar, there is not a spreader available that can meet the required capacity, which is 58,667 lb (26.61 ton). Therefore, the lengths of the slings at level 3 are increased to the next longer sling in the database (i.e., 30 ft) and the value of S_R is updated to 372 in (9.45 m). Consequently, the angles of slings above the spreader bar are increased to θ_L = 58.69° and θ_R = 66.67°. Considering the updated angles, a 372 in (9.45 m) long spreader bar with the capacity of 67,200 lb (30.48 tonne) is selected. The required capacity of the slings at the third level is 37,383 lb (16.96 tonne). Then, the suitable sling (i.e. Ø1-1/2 in × 30 ft) is selected from the database, which has a 42,000 lb (19.05 tonne) capacity.

As the COG is offset from the COM in both X and Y directions, sling length adjustment is required at the second and third levels to balance the load. The *RAI* at the second level and third level is 15.92 in (40.4 cm) and 27.81 in (70.6 cm), respectively. Therefore, two 35-tonne shackles that have 15.5 in (39.4 cm) inside length in total are attached to the slings at the second level; and a combination of one 35-ton and two 55-tonne shackles, which have a total 28.82 in (73.2 cm) inside length, are added to the sling at the third level.

The design of the 2-point pick segment in the middle of the rigging assembly begins with calculating the total height of the 4-point pick segment. Based on the selected rigging components, the height of the 4-point pick segment is 18.67 m. The length of drop slings is set and fixed to the

length of those used in the 4-point pick segments (i.e. 10 ft.). Using the algorithm of designing 2-point pick segments (see Fig. 14), all of the feasible slinging arrangements and the suitable turnbuckle is generated. The results of the 2-point pick rigging assembly design are represented in Fig X. This figure shows all of the iterations in the inner and outer loop of the design algorithm which results in three acceptable slinging arrangements.

Fixed parameters (in)		
SL_{1st} = 120	$Min(TB_L)$ = 49.37	$Max(SL_{DB})$ = 480
$H_{desired}$ = 735.97	$Max(TB_L)$ = 72.05	$Min(SL_{DB})$ = 120

SL_{2nd} (in)	SL_{3rd} (in)	H_{slings} (in)	H_{remain} (in)	$H_{Remain} > Min(TB_L)$	$H_{Remain} < Max(TB_L)$	$SL_{3rd} < Max(SL_{DB})$	$SL_{2nd} < Max(SL_{DB})$	Accepted
240	120	452.99	282.98	Yes	No	Yes	Yes	No
240	180	483.20	252.77	Yes	No	Yes	Yes	No
240	240	513.30	222.67	Yes	No	Yes	Yes	No
240	300	543.36	192.61	Yes	No	Yes	Yes	No
240	360	573.40	162.57	Yes	No	Yes	Yes	No
240	420	603.43	132.54	Yes	No	Yes	Yes	No
240	480	633.45	102.52	Yes	No	No	Yes	No
300	120	515.86	220.11	Yes	No	Yes	Yes	No
300	180	546.01	189.96	Yes	No	Yes	Yes	No
300	240	576.11	159.86	Yes	No	Yes	Yes	No
300	300	606.18	129.79	Yes	No	Yes	Yes	No
300	360	636.22	99.75	Yes	No	Yes	Yes	No
300	420	666.25	69.72	Yes	Yes	Yes	Yes	Yes
360	120	574.17	161.8	Yes	No	Yes	Yes	No
360	180	604.38	131.59	Yes	No	Yes	Yes	No
360	240	634.48	101.49	Yes	No	Yes	Yes	No
360	300	664.54	71.43	Yes	Yes	Yes	Yes	Yes
420	120	635.48	100.49	Yes	No	Yes	Yes	No
420	180	665.69	70.28	Yes	Yes	Yes	Yes	Yes
480	120	695.98	39.99	No	Yes	Yes	No	No

Fig. 23. Results of the 2-point pick segment design algorithm

Finally, 3D model of the rigging assembly is created by the 3D visualizer module. In the 3D model, an incompatibility between lifting points (lifting lugs) of the module and the shackles attached to them was encountered, as the selected shackles were relatively small, even though they

were able to meet the required capacity. Therefore, these shackles were replaced by 25-tonne shackles manually. Fig. 24, represents the final rigging assembly while the second possible slinging arrangement of the 2-point pick segment is used.

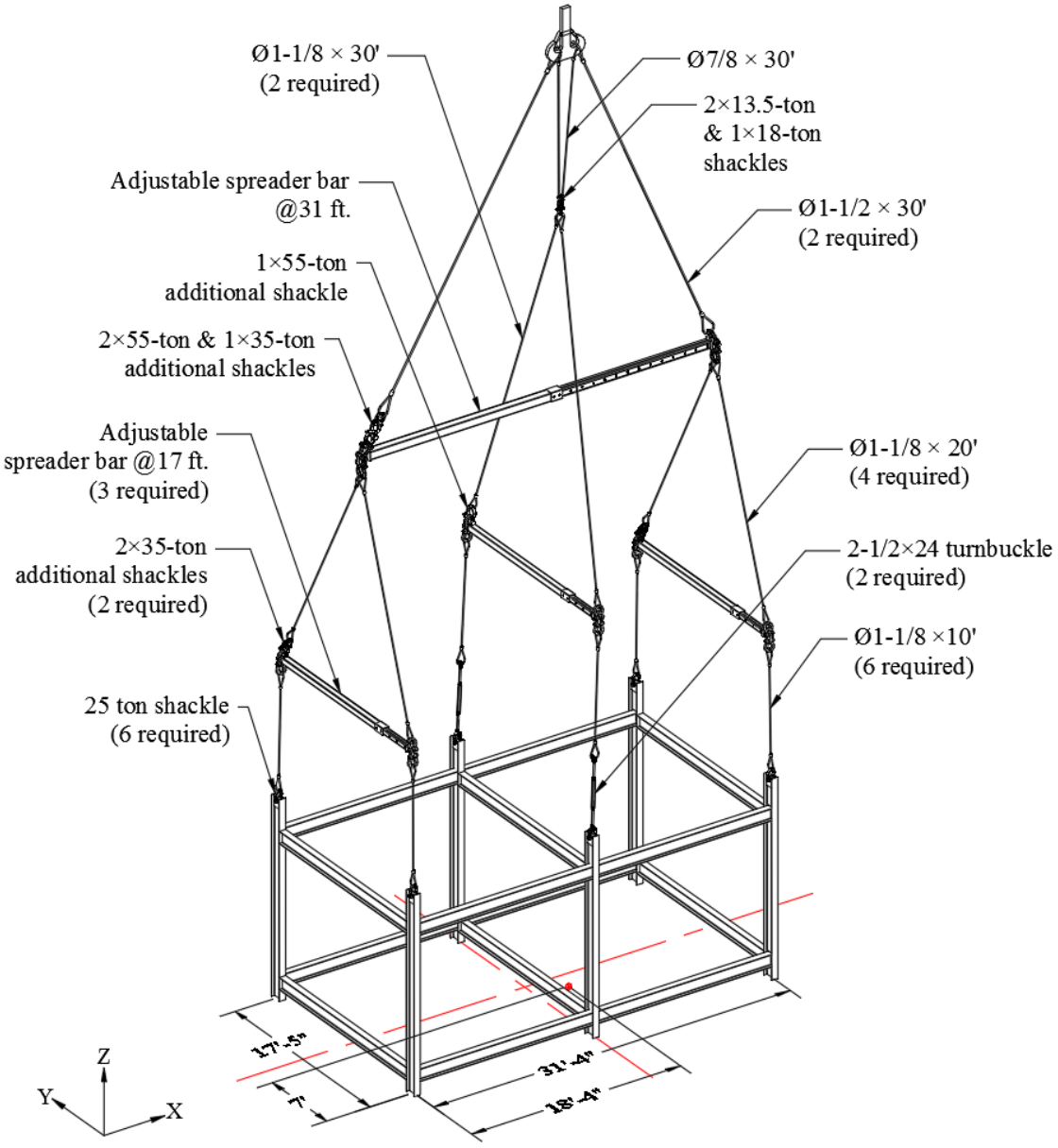

Fig. 24. Final result of the 6-point pick rigging assembly

4.2 Case Study 2

The other module which is used as a case study is a 40,000 lb (18.1 tonne) 4-point pick module with the length of 182 in (4.62 m) and width of 90 in (2.29 m). The COG of the module is offset from the bottom left corner of the module (P1) by 105 in (2.67 m) and 60 in (1.52 m) in X and Y direction, respectively. As shown in Fig. 25 the width of the hook and the maximum acceptable drop sling angle is determined by the user as 17 in (0.43 m) and 1.5°.

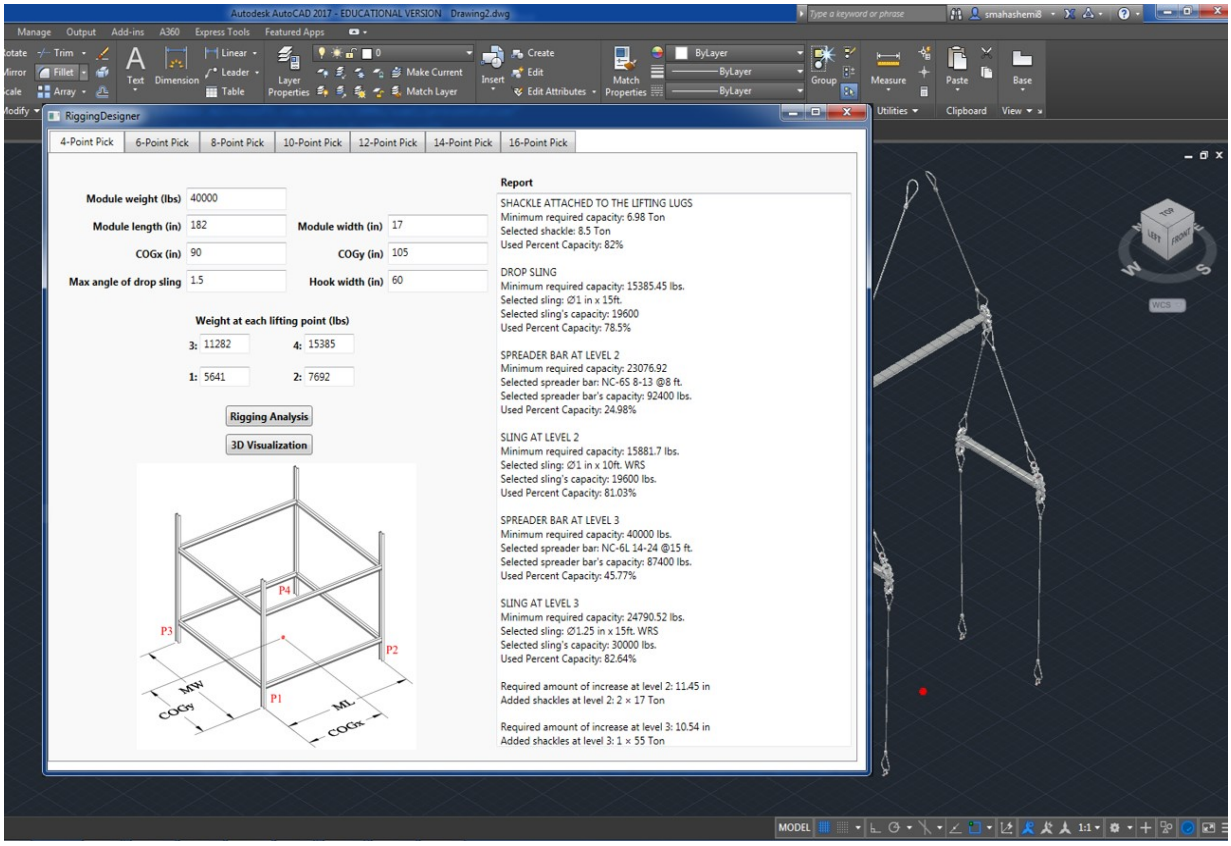

Fig. 25. The user interface of the proposed methodology

Assuming that the COG is at the center of module, a preliminary rigging assembly is deigned by the designer module to provide the input data for the solver module. The selected rigging components of the preliminary rigging assembly are shown in Table 3.

Table 3. Selected rigging components for the preliminary rigging assembly

Rigging component	Description
Shackle at the lifting points	4.75-tonne (inside length = 2.81 in)
Sling length at the first level (drop sling)	10 ft.
Sling length at the second level	10 ft.
Sling length at the third level	15 ft.
Spreader bar length at the second level	8 ft.
Spreader bar length at the third level	15 ft.

In order to calculate the angle of slings attached to the spreader bar at level 2 (represented as the red plane in Fig. 26), based on the preliminary design and inputs of the system, the initial value of S_R, SB_L, M, *ofst,* and H_W as the known parameters of the solver module is determined as S_R = 128.75 in (3.27 m), SB_L = 96 in (2.44 m), S_B = 132 in (3.35 m), M = 90 in (2.29 m), *ofst* = 30 in (0.76 m), and H_W = 0. By calling task 1 of the solver module, the sling angles are computed as α = 0.9°, β = 1.7°. Since the maximum acceptable drop sling angle (1.5°) is not satisfied, the drop slings are increased by 5 ft. (length interval of the slings in the database). The solver module is called to recalculate the sling angles using the update input data. The updated value of input and output parameters is shown in Fig. 26.

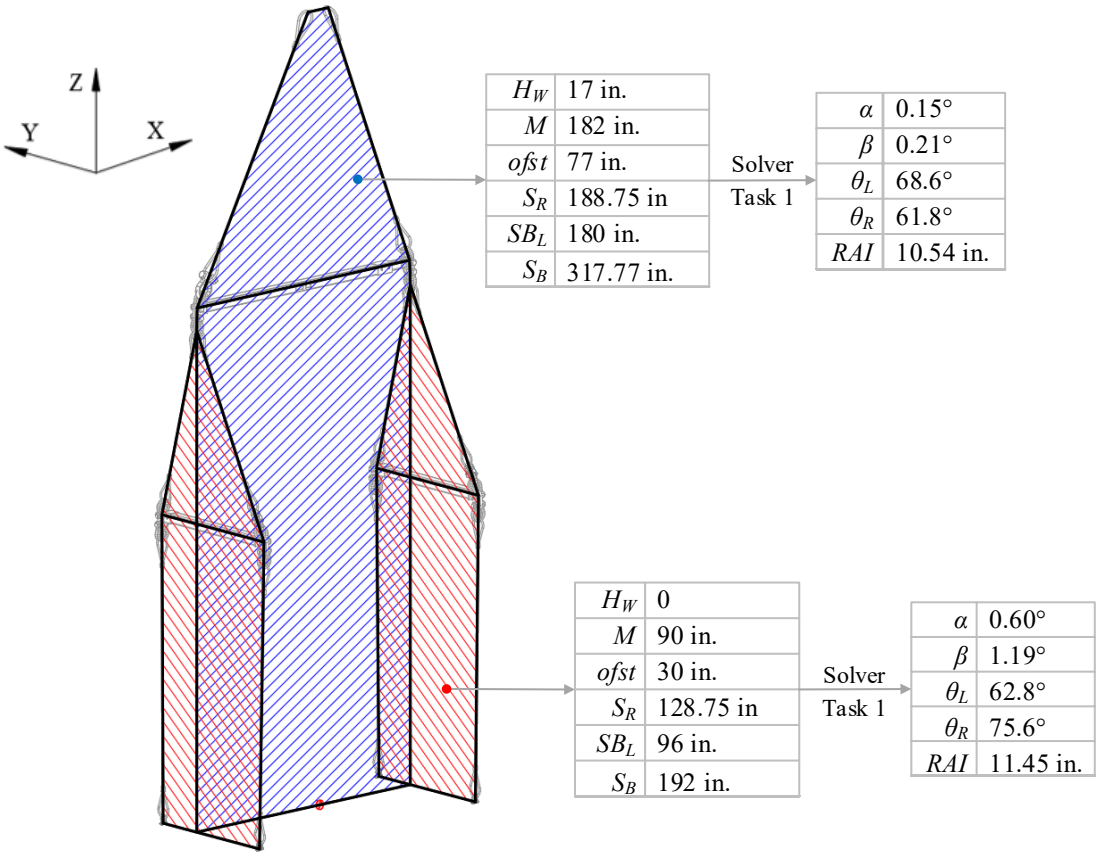

Fig. 26. Calculations of sling angles and *RAI* in two-dimensional planes

Based on the sling angles and the amount of weight at the lifting points, the required capacity of the shackles at the lifting points, drop slings, spreader bar, and the slings at level 2 are calculated and the suitable slings and spreader bar are selected from the database as shown in Table 4. It should be noted that, the selected sling length in the preliminary design is long enough for the required capacity of the spreader bar and there is no need to increase the length of sling in order to gain higher capacity of the spreader bar.

Similarly, the angle of slings located at the third level of the rigging assembly are calculated by the solver module in the plain containing the spreader bar at this level (represented as the blue plain in Fig. 26). Therefore, based on the computed sling angles, the required capacity of slings and spreader bar at level is determined and the suitable slings and spreader bar is selected from the

database as shown in Table 4.

Table 4. the required and rated capacity of the selected rigging components

Rigging component	Required capacity	Rated capacity
Shackles at the lifting points	6.98 tonne	8.5 tonne
Sling at the first level	15,385 lb (6.98 tonne)	19,600 lb (8.89 tonne)
Sling at the second level	15,882 lb (7.2 tonne)	19,600 lb (8.89 tonne)
Sling at the third level	24,790 lb (11.24 tonne)	30,000 lb (13.61 tonne)
Spreader bar at the second level	23,077 lb (10.47 tonne)	92,400 lb (41.91 tonne)
Spreader bar at the third level	40,000 lb (18.14 tonne)	87,400 lb (39.64 tonne)

In order to balance the module in both X and Y direction, additional shackles are required to be added above the spreader bars at both level two and three. The RAI at level two is calculated by task 2 of the solver module as 11.45 in (29.1 cm). So, two 17-tonne shackles which have 11.5 in (29.2 cm) inside length in total are mounted above the spreader bar at level two to balance the module in Y direction. The RAI at level three is calculated as 10.54 in (26.8 cm). Therefore, a 55-tonne shackle which has 10.5 in (26.7 cm) inside length is mounted to above the spreader bar at level three to balance the load in X direction. Fig. 27, represents the final 3D model of the rigging assembly.

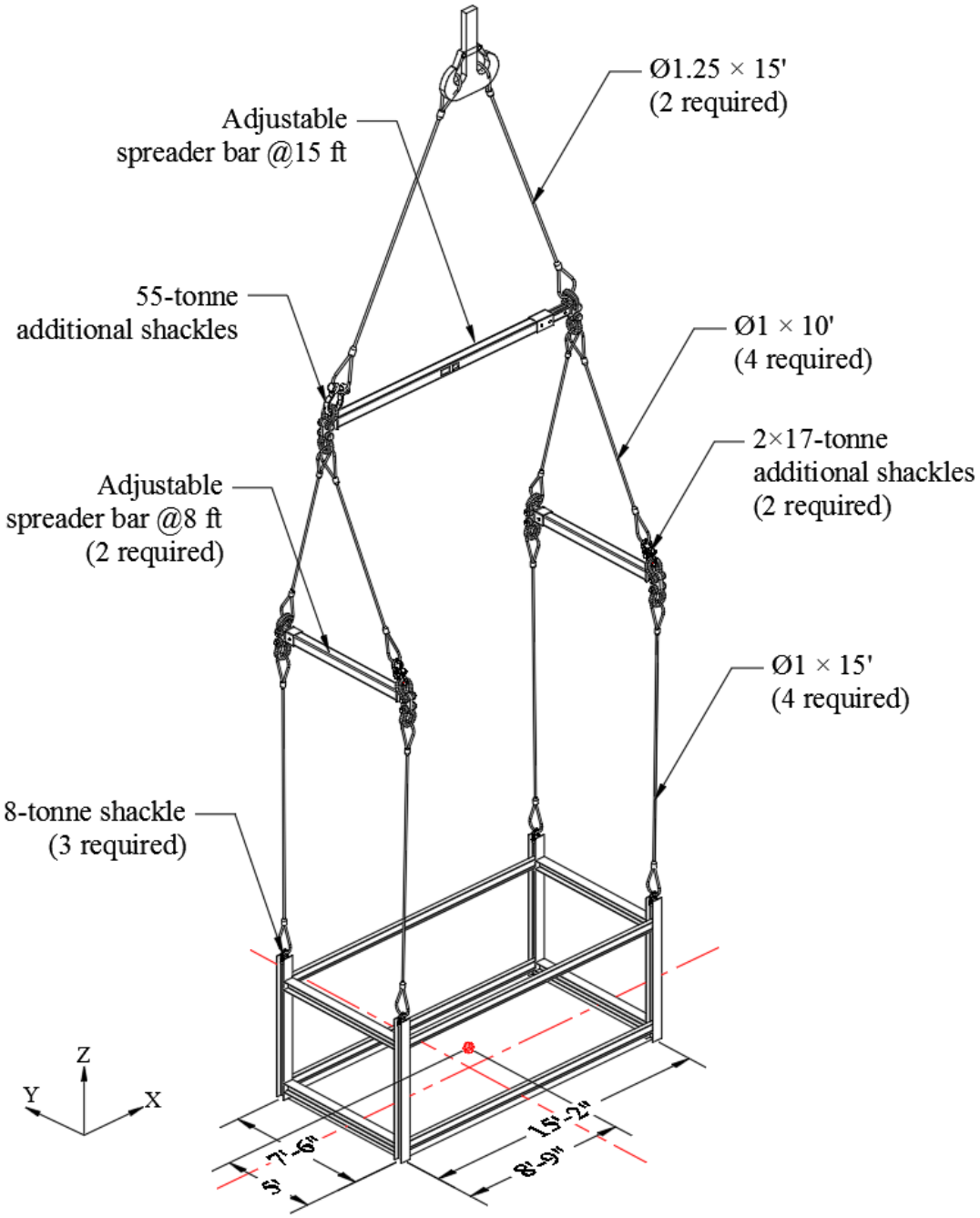

Fig. 27. Final result of the 4-point pick rigging assembly

Chapter 5: Future Works

The proposed methodology is subject to some limitations and requires further development. The current system uses an Excel database which not only is prone to accidental changes to data while developing the database but also makes the automated system relatively slows. These issues therefore could be addressed by developing a SQL database which is faster and more maintainable.

Another limitation of the current system is that the module information (i.e. weight, dimensions, center of gravity position) is required to be entered by the user manually. Considering that the number of modules in major refinery projects may reach over 100, manually entering information for each module and then running the system for each individual one could be a tedious and prolonged process. A better approach in regards of this issue could be creating a database of modules information and developing the proposed system in a way to collect the information from the modules database to automatically design and visualize the rigging assembly for the entire modules. In this context, implementing Building Information Modelling (BIM) process could also be considered as further development of the framework. Using BIM tools, the modules and the rigging assemblies can be managed and designed in an integrated environment. In that case, other parameters such as scheduling and cost could be factored in for making decisions in the design and planning phase of the lifting projects.

The current system selects the same rigging components at each level of the rigging assembly since only the maximum load at each level is considered as the required capacity. Therefore, the output of the system is an over designed rigging assembly. In this context, structural analysis could be implemented in the future works in order to determine the actual forces applied to each rigging component and select the suitable rigging components according to the actual required capacity.

As it was explained in the 2-point pick segments, in the current system, the design alternatives are generated by changing the length of slings at different levels of the configuration in a nested loop and the final decision is to be made by the user to use one of the design alternatives. This issue could be addressed by optimizing the design process so that only one rigging assembly is generated which is the optimal one. The optimization objectives could be the weight of the rigging assembly, used capacity of the rigging components and the way that the load is distributed throughout the segment.

The heights of lifting points on some modules are not in the same elevation. In designing the rigging assembly for those modules, the sling length at the first level needs to be adjusted to bring all of the lifting points to the same elevation. Also, for some modules, especially those which are lifted from the bottom and their lifting points are installed on their beams, vertical lift may not be essential. Therefore, for those modules inclined slings are used at the first level of their rigging assembly. The current system cannot be used to design the rigging assembly of the aforementioned modules.

Chapter 6: Conclusion

Prior to lifting heavy modules at industrial sites, crane lift studies including crane selection, crane location, crane support system, rigging assembly design, and crane motion planning are essential to ensure that the modules are lifted and erected safely and efficiently. As one of the main components of a crane lift study, the rigging assembly design involves tedious, complex, and time-consuming tasks such as calculating the sling angles, determining the required capacity of the rigging components, selecting suitable rigging components, and creating the 3D model of the designed rigging assembly. These tasks become more complicated when the module's center of gravity is offset from the center of module. Rigging assemblies are required to be designed in a way to ensure that the modules are lifted vertically and maintained in a level position during the lift. Lifting modules unevenly increases the risk of module tilting and deflection, and, more importantly, the risk of rigging failure as a result of unexpected distribution of the load throughout the rigging assembly. Poorly designed rigging assemblies are only detected at the job site when the module does not raise evenly at the beginning of the lift, which results in wasted time and productivity loss, as the assembled components have to be unrigged and properly adjusted. In this respect, this thesis has proposed an automated mathematical-based rigging assembly design system to assist lift engineers by automating the design and visualization of rigging assemblies. The proposed framework consists of the following three elements: (*i*) the solver, which performs two tasks: calculating the sling angles at each level of the rigging assembly through solving a system of nonlinear equations, and finding the optimal size and number of shackles that are attached to slings to increase their lengths; *(ii)* the designer, which calculates the required capacity of the rigging components based on the module information and selects suitable rigging components that

meet the required capacity from the database considering their availability; and *(iii)* the 3D visualizer, which creates a 3D model of the rigging assembly in the AutoCAD platform to identify whether the selected rigging components can be properly assembled in real life. A 6-point pick and a 4-point pick module were used as a case study to demonstrate the validity and effectiveness of the proposed framework. Also, the framework was tested on 50 modules, which resulted in saving almost 42 hours (50 minutes per module) in total and eliminating manual design errors, which can happen at a rate of approximately 5 to 10%.

References

[1] G. P. Burke, R. C. Miller, Modularization speeds construction, Power Engineering 102 (1) (1998) 20–23.

[2] L. Westover, J. Olearczyk, U. Hermann, S. Adeeb, Y. Mohamed, Analysis of rigging assembly for lifting heavy industrial modules, Canadian Journal of Civil Engineering 41 (6) (2014) 512–522.

[3] J. Olearczyk, Z. Lei, B. Ofrim, S. Han, M. Al-Hussein, Intelligent crane management algorithm for construction operation, proceedings, International Association for Automation and Robotics in Construction (IAARC), Oulu, Finland, 2015, pp. 1-8.

[4] H. Taghaddos, U. Hermann, A. Abbasi, Automated crane planning and optimization for modular construction, Automation in Construction 95 (2018) 219–232.

[5] C.-S. Cho, F. Boafo, Y.-J. Byon, H. Kim, Impact analysis of the new OSHA cranes and derricks regulations on crane operation safety, KSCE Journal of Civil Engineering 21 (1) (2016) 54–66.

[6] J. Olearczyk, M. Al-Hussein, A. Bouferguene, Evolution of the crane selection and on-site utilization process for modular construction multilifts, Automation in construction 43 (2014) 59–72.

[7] S. Han, S. Hasan, A. Bouferguene, M. Al-Hussein, J. Kosa, An integrated decision support model for selecting the most feasible crane at heavy construction sites, Automation in Construction 87 (2018) 188–200.

[8] D. Wu, Y. Lin, X. Wang, X. Wang, S. Gao, Algorithm of crane selection for heavy lifts, Journal of Computing in Civil Engineering 25 (1) (2011) 57–65.

[9] Y. Lin, H. Yu, G. Sun, P. Shi, Lift path planning without prior picking/placing configurations: Using crane location regions, Journal of Computing in Civil Engineering 30 (1) (2014) 04014109.

[10] S. Han, Z. Lei, A. Bouferguene, M. Al-Hussein, U. Hermann, 3d visualization-based motion planning of mobile crane operations in heavy industrial projects, Journal of Computing in Civil Engineering 30 (1) (2014) 04014127.

[11] Z. Lei, S. Han, A. Bouferguene, H. Taghaddos, U. Hermann, M. Al-Hussein, Algorithm for mobile crane walking path planning in congested industrial plants, Journal of Construction Engineering and Management 141 (2) (2014) 05014016.

[12] H. R. Reddy, K. Varghese, Automated path planning for mobile crane lifts, Computer-Aided Civil and Infrastructure Engineering 17 (6) (2002) 439– 448.

[13] Z. Lei, H. Taghaddos, S. Han, A. Bouferguene, M. Al-Hussein, U. Hermann, From AutoCAD to 3ds max: An automated approach for animating heavy lifting studies, Canadian Journal of Civil Engineering 42 (3) (2015) 190–198.

[14] S. H. Han, S. Hasan, A. Bouferguene, M. Al-Hussein, J. Kosa, Utilization of 3d visualization of mobile crane operations for modular construction on-site assembly, Journal of Management in Engineering 31 (5) (2014) 04014080.

[15] S. Han, A. Bouferguene, M. Al-Hussein, U. R. Hermann, 3d-based crane evaluation system for mobile crane operation selection on modular-based heavy construction sites, Journal of Construction Engineering and Management 143 (9) (2017) 04017060.

[16] H. Taghaddos, A. Eslami, U. Hermann, S. AbouRizk, Y. Mohamed, Auction-based simulation for industrial crane operations, Automation in Construction 104 (2019) 107–119.

[17] K. D. Roy, A. K. Dev, S. Aksu, Installation engineering of topside modules on ship shaped offshore floating structures, Advanced Maritime Engineering Conference (AMEC), Singapore, 2010.

[18] Anderson J. K. Rigging Engineering Basics, 1(1), ITI Bookstore, Woodland, Washington 98674, (2013).

[19] The Crosby Group LLC. Crosby General Catalogue. 2801 Dawson Rd., Tulsa, OK 74110, (2017).

[20] M.-T. Sam, Offshore heavy lift rigging analysis using spreadsheet, Practice Periodical on Structural Design and Construction 14 (2) (2009) 63–69.

[21] R. Longman, F. Freudenstein, Stability analysis of lifting rigs part 1: Necessary and sufficient conditions, Journal of Engineering for Industry 97 (2) (1975) 532–536.

[22] P.-Y. Chen, Z.-Y. Zhuang, C.-M. Chang, S.-C. Kang, A numerical model for the attitude manipulation of twin-hoisted object, Proceedings, International Association for Automation and Robotics in Construction (IAARC), Berlin, Germany, 2018, pp. 219-223.

[23] K.-L. Lin, C. T. Haas, Multiple heavy lifts optimization, Journal of construction engineering and management 122 (4) (1996) 354–362.

[24] C. Bennett, S. Ditlinger, Bechtel automated lift planning system, in: Robotics for challenging environments, (19)94, p. 401.

[25] K. Varghese, P. Dharwadkar, J. Wolfhope, J. T. O'Connor, A heavy lift planning system for crane lifts, Computer-Aided Civil and Infrastructure Engineering 12 (1) (1997) 31–42.

[26] 3D Lift Plan software, A1A software LLC, < http://www.a1asoftware.net/about.html>, Accessed date: May, 2019.

[27] CRANEbee Software, CRANIMAX Software development and distribution company, <https://www.cranimax.com/> Accessed date: May, 2019.

[28] kranXpert software, Markus Scholl, < https://www.kranxpert.de/>, Accessed date: May, 2019.

[29] S. Hashemi, S. Han, J. Olearczyk, A. Bouferguene, M. Al-Hussein, J. Kosa, Automated mathematical-based design framework for the selection of rigging configuration, Proceedings, International Association for Automation and Robotics in Construction (IAARC), Banff, Canada, 2019, pp. 172-178.